

4

TECHNICAL REPORT
NADC 82047-60



AD A119627

ADVANCED FLIGHT CONTROL ACTUATION SYSTEM (AFCAS - E/P)

**Fabrication and Design Verification Testing of a
Dual Mode Electro/Pneumatic Actuator for the
T-2C Aircraft**

Wallace Kinetyo

Bendix Corporation
Flight Systems Division
Teterboro, New Jersey

APRIL 1982

FINAL REPORT FOR PERIOD SEPTEMBER 1978 - APRIL 1981

APPROVED FOR PUBLIC RELEASE:
DISTRIBUTION UNLIMITED

PREPARED FOR

NAVAL AIR DEVELOPMENT CENTER 6013
WARMUNSTER, PENNSYLVANIA 18974

DTIC
ELECTE
SEP 27 1982
S D
B

DTIC FILE COPY

UNCLASSIFIED

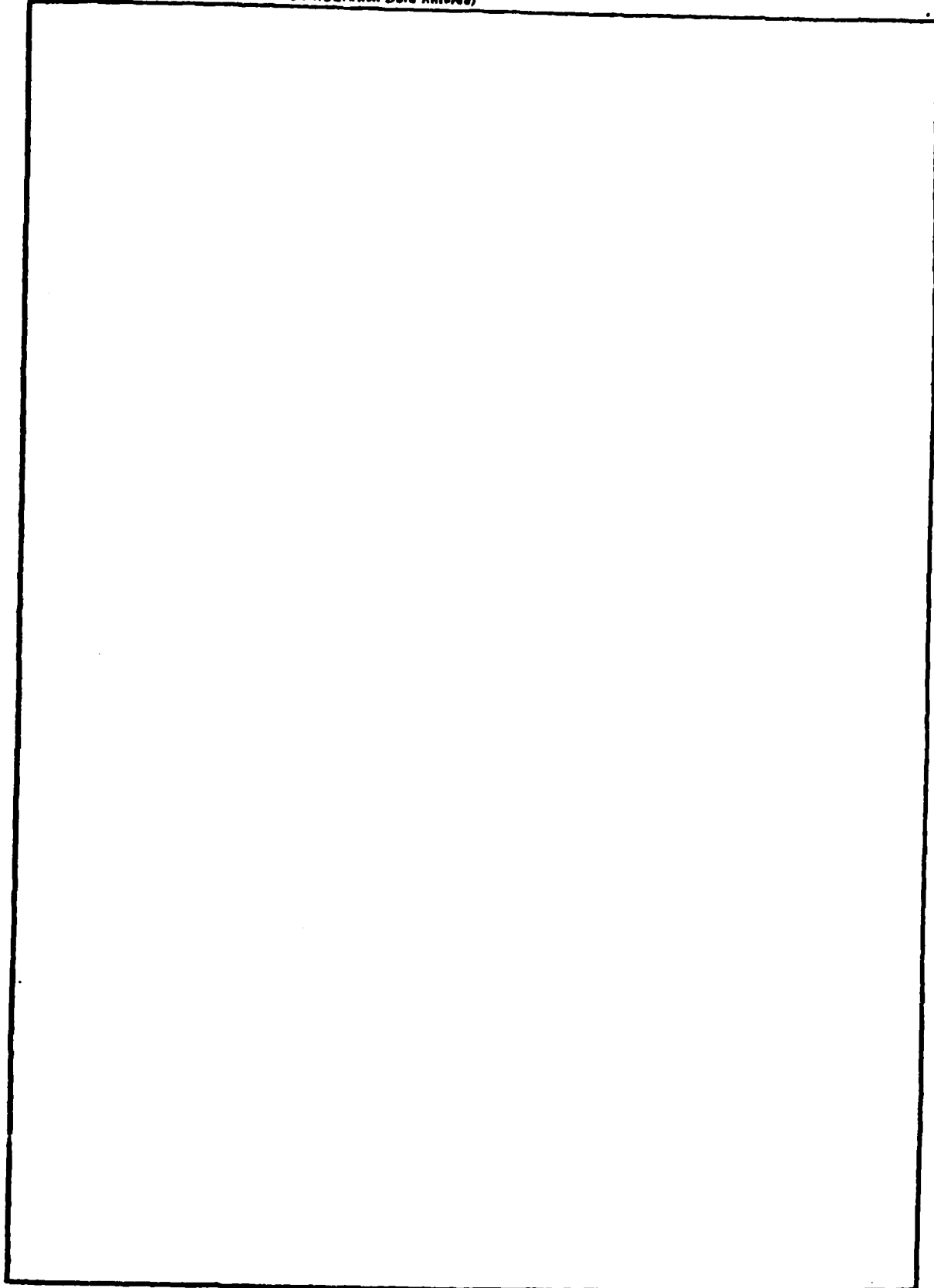
SECURITY CLASSIFICATION OF THIS PAGE (When Data Entered)

REPORT DOCUMENTATION PAGE		READ INSTRUCTIONS BEFORE COMPLETING FORM
1. REPORT NUMBER NADC 82047-60	2. GOVT ACCESSION NO. AD-A119627	3. RECIPIENT'S CATALOG NUMBER
4. TITLE (and Subtitle) Fabrication and Design Verification Testing of a Dual Mode Electro/Pneumatic Actuator for the T-2C Aircraft		5. TYPE OF REPORT & PERIOD COVERED Final Report Sept. 1978 - April 1981
		6. PERFORMING ORG. REPORT NUMBER
7. AUTHOR(s)		8. CONTRACT OR GRANT NUMBER(s) N62269-78-C-0247
9. PERFORMING ORGANIZATION NAME AND ADDRESS Bendix Corporation Flight Systems Division Teterboro, New Jersey 07608		10. PROGRAM ELEMENT, PROJECT, TASK AREA & WORK UNIT NUMBERS 622-41N-F41400
11. CONTROLLING OFFICE NAME AND ADDRESS Naval Air Development Center (6013) Warminster, Pennsylvania 18974		12. REPORT DATE April, 1982
		13. NUMBER OF PAGES
14. MONITORING AGENCY NAME & ADDRESS (if different from Controlling Office) AIR 340D and 5303 Naval Air Systems Command Department of the Navy Washington, DC 20361		15. SECURITY CLASS. (of this report) Unclassified
		15a. DECLASSIFICATION/DOWNGRADING SCHEDULE
16. DISTRIBUTION STATEMENT (of this Report) Approved for public release, distribution unlimited.		
17. DISTRIBUTION STATEMENT (of the abstract entered in Block 20, if different from Report)		
18. SUPPLEMENTARY NOTES		
19. KEY WORDS (Continue on reverse side if necessary and identify by block number) Dual Mode Electro/Pneumatic Actuator, Pneumatic Motor, Servo Valve, Pneumatic Commutation, Epicyclic Gear Transmission, Low inertia		
20. ABSTRACT (Continue on reverse side if necessary and identify by block number) Report of the fabrication and design verification testing of a Dual Mode Electro/Pneumatic Actuator. Pneumatic mode open loop operation and control verified. Torque/Speed performance less than design goal due to excessive gear separation force.		

DD FORM 1473 1 JAN 73 EDITION OF 1 NOV 68 IS OBSOLETE

UNCLASSIFIED
SECURITY CLASSIFICATION OF THIS PAGE (When Data Entered)

SECURITY CLASSIFICATION OF THIS PAGE(When Data Entered)



SECURITY CLASSIFICATION OF THIS PAGE(When Data Entered)

EXECUTIVE SUMMARY

1.0 INTRODUCTION

This report presents the results of an effort conducted at Bendix Flight Systems Division, Teterboro, New Jersey, in compliance with Contract No. 2269-78-C-0247 awarded by the Naval Air Development Center Warminster, Pennsylvania to fabricate, test, and deliver one Dual Mode Electro/Pneumatic Actuator for the T-2C aircraft.

Design details and performance predictions for the actuator were accomplished in a Bendix-FSD study completed earlier under NADC contract No. N62269-77-C-0171 and documented in a final report entitled "Feasibility Investigation of an Electro/Pneumatic Dual Power Driven Concept" (NADC Technical Report 77001-60) dated June, 1978.

The scope of this report deals with the fabrication and assembly events of the hardware and with test methods and results of the completed actuator.

2.0 BACKGROUND

Computer studies have demonstrated that actuator systems based on a dual mode concept have greater survivability than single mode limited actuators. Operation within performance specifications is maintained despite the loss of either of the dissimilar operational modes. No interruption of control occurs during or after such power loss.

The Dual Mode Electro/Pneumatic Actuator developed under this program embodies a unique combination of actuator principles whereby both electrical and pneumatic control may be accomplished within a single rotary actuator assembly. Inherently low reflected inertia of this design offers a high performance capability.

The dual nature of the actuator provides that distinct advantage in control survivability. Upon electric power failure, full control can be maintained with the pneumatic mode operating from the aircraft engine bleed air. The actuator was designed to allow simultaneous dual operation as its primary mode. Simulation studies already conducted have verified the related

<input checked="" type="checkbox"/>
<input type="checkbox"/>
<input type="checkbox"/>

PER LETTER



Distribution/	
Availability Codes	
Avail and/or	
Dist Special	
A	

system implications in dual operation, individual mode operation, and final reversion to bleed air control and found all modes practical and advantageous toward control system survivability.

3.0 FINDINGS

A dual mode electro/pneumatic actuator was fabricated and assembled in accordance with Bendix/FSD drawing no. 3854020-1 (Figure 1) and open-loop, no load tests were conducted on the completed unit. Figures 2 and 3 are photos of the actuator.

No major problems were encountered during the hardware procurement phase other than some difficulty in locating suitable vendors to fabricate the more complex parts.

Air flow measurements of the servo-valve flow trim assembly indicated a lower flow rate and threshold sensitivity than that specified. Its performance capability, however, was considered more than adequate to accommodate the expected actuator performance level based on initial test results of the actuator.

Assembly of the hardware into a completed actuator was essentially a simple, straight forward operation. Some difficulties, however, were encountered on initial assembly in achieving a proper fit of the manifold plates to the stator. Minor re-work of the gaskets, stator, and manifold plates alleviated the interference.

Open loop tests of the actuator indicated actual performance to be less than design goals. No load speed and stall torque were measured at 60% and 30%, respectively, of the predicted levels. The major cause of the performance short fall was identified as excessive mechanical interference in the epicyclic gear mesh created by a gear separation force of a magnitude previously unaccounted for. Constraint of the rotor to oppose the gear separation force will be required to allow higher ratio actuators of this type to develop maximum torque and speed. Adoption of an eccentric bearing rotor support design is recommended to effect a correction.

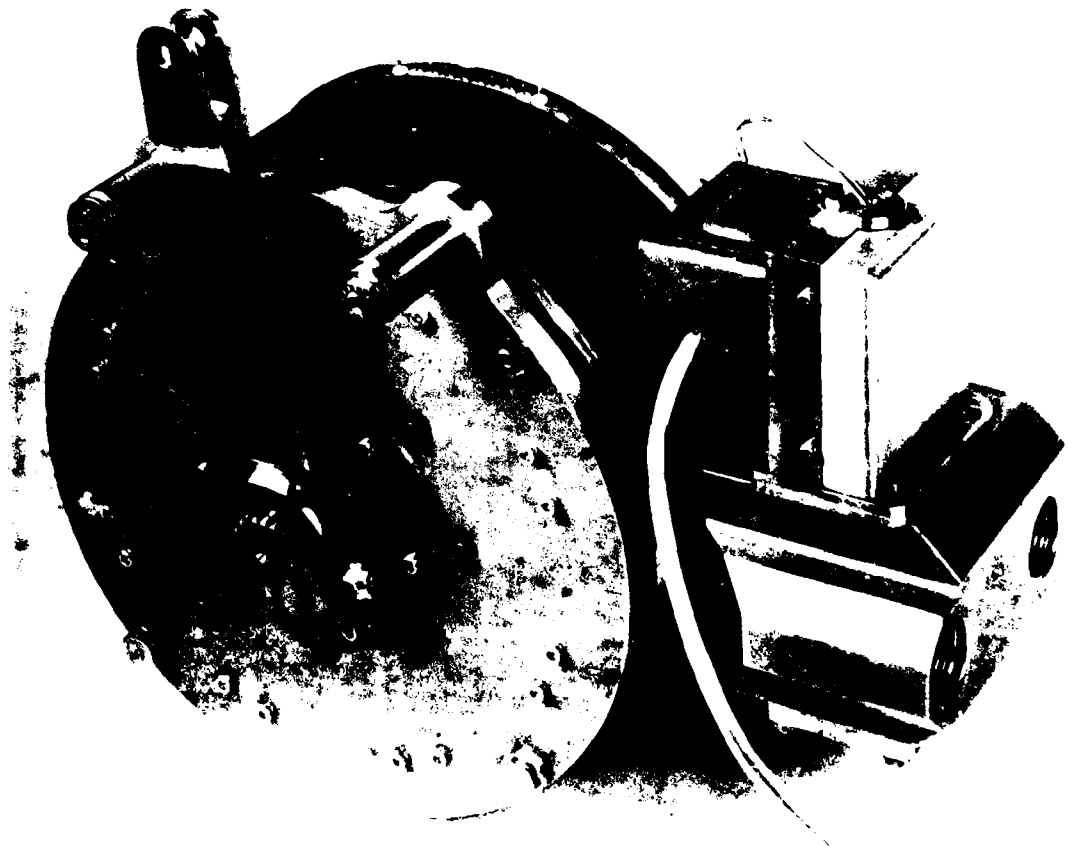
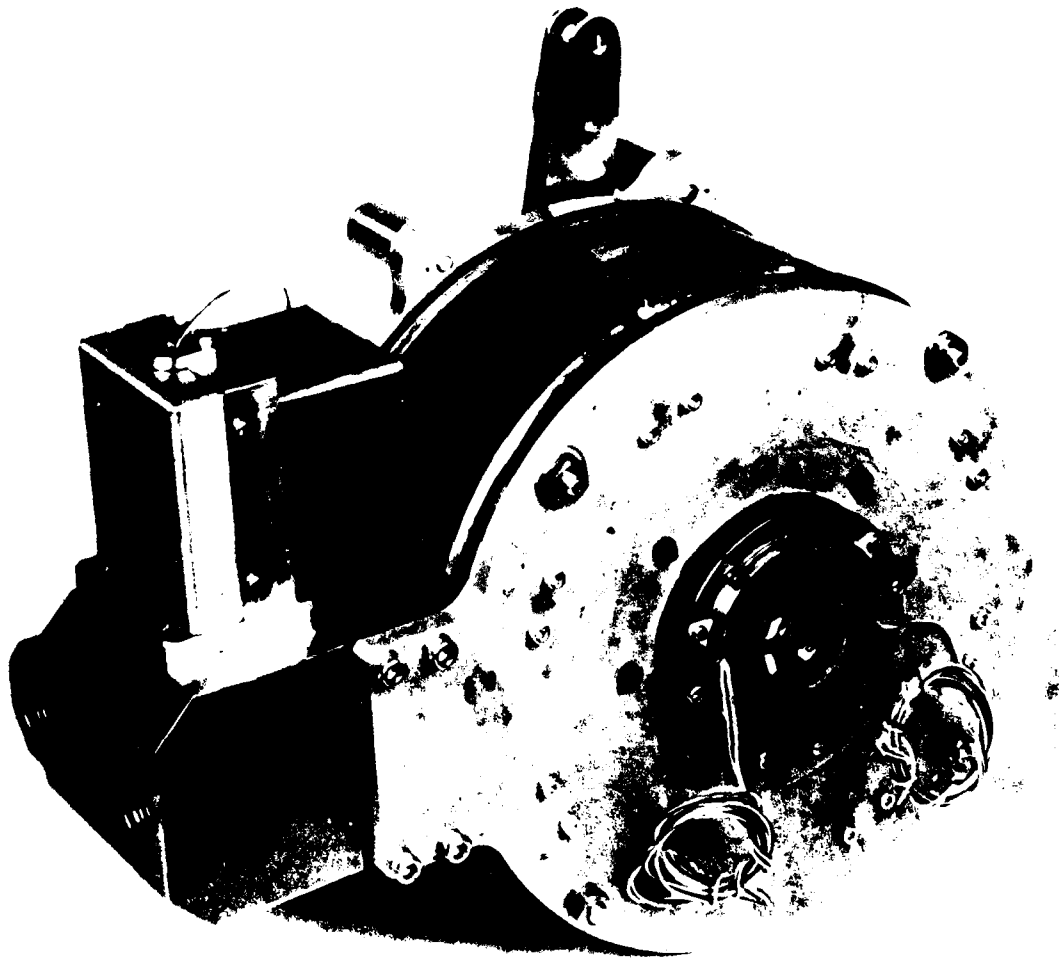


FIGURE 2 ELECTRO/PNEUMATIC ACTUATOR

FIGURE 2



ELECTRO-PNEUMATIC ACTUATOR

FIGURE 3

TABLE OF CONTENTS

<u>SECTION</u>	<u>TITLE</u>	<u>PAGE</u>
	Executive Summary	1
1.0	Introduction	1
2.0	Background	1
3.0	Findings	2
4.0	Discussion	9
4.1	Fabrication	9
4.1.1	Materials	9
4.1.2	Processes	9
4.1.3	Sub Assemblies	9
4.2	Assembly	9
4.2.1	Procedure	10
4.2.2	Problems	10
4.3	Test Methods and Results	17
4.3.1	Pneumatic Mode	17
4.3.1.1	Servo Valve Mechanism	17
4.3.1.2	Actuator	19
4.3.1.2.1	Flow Losses	26
4.3.1.2.2	Torque/Speed	26
4.3.2	Electric Mode	28
4.3.2.1	Insulation Resistance	28
4.3.2.2	Torque/Speed	28
4.3.2.3	Power Consumption	32
4.3.3	Transient Response	32
4.4	Teardown Inspection	32
4.5	Performance Analysis	39
5.0	Conclusions and Recommendations	42
APPENDIX A	Electro Pneumatic Actuator Dual Mode Parts List	46

LIST OF ILLUSTRATIONS

<u>FIGURE</u>	<u>TITLE</u>	<u>PAGE</u>
1	Electro/Pneumatic Actuator Dual Mode Drawing	3
2	Electro/Pneumatic Actuator Photo	4
3	Electro Pneumatic Actuator Photo	5
4	Stator Assembly Photo	11
5	Left Manifold Plate - Left Pneumatic Transfer Plate Photo	12
6	Roller Bearings - Ring Gear Photo	13
7	Rotor Photo	14
8	Gears - Rotor - Stator Assembly Photo	15
9	Right Manifold Plate - Right Pneumatic Transfer Plate Photo	16
10	Dual Mode Electro/Pneumatic Actuator Bench Test Hook-up Drawing	18
11	Servo Valve Flow Trim Test Fixture Photo	20
12	Servo Valve Mechanism Airflow Test Diagram	21
13	Servo Valve Mechanism Air Flow Graph	22
14	Pneumatic Mode Test Set-up Electro/Pneumatic Actuator Photo	23
15	Pneumatic Mode Test Set-Up Electro/Pneumatic Actuator Photos	24
16	Electro/Pneumatic Actuator Pneumatic Mode Open Loop Test Diagram	25
17	Pneumatic Mode Torque Test Set-Up Electro/Pneumatic Actuator Photo	27
18	Electro/Pneumatic Actuator Pneumatic Mode Torque/Speed Curve	29
19	Pneumatic and Electric Mode Open Loop Test Set-Up Photo	30
20	Electro/Pneumatic Actuator Electric-Mode Open Loop Test Diagram	31

LIST OF ILLUSTRATIONS

<u>FIGURE</u>	<u>TITLE</u>	<u>PAGE</u>
21	Electro/Pneumatic Actuator Electric Mode Torque-Speed Curve	33
22	Pneumatic and Electric Mode Open Loop Transient Response Test Set-Up Photo	34
23	Electro/Pneumatic Actuator Open Loop Transient Response Test Diagram	35
24	Electro/Pneumatic Actuator Pneumatic Mode Open Loop Transient Response Recording	36
25	Electro/Pneumatic Actuator Pneumatic Mode Open Loop Transient Response Recording	37
26	Electro/Pneumatic-Actuator Electric Mode Open Loop Transient Response Recording	38
27	8 Pole High Ratio Actuator Sketch	44
28	4 Pole High Ratio Actuator Sketch	45

4.0 DISCUSSION

4.1 FABRICATION

4.1.1 Materials

Initial design drawings specified the use of 18 Nickel 350 Maraging Steel for the actuator gearing. Procurement cost of this material in bulk form for the small quantities involved was prohibitive. A suitable substitute material, 18 Nickel 300 Maraging Steel, was found to be available at a reasonable cost and was used to fabricate the affected parts.

4.1.2 Processes

Cracks developed in the rotor during the carburizing phase of its fabrication. Discussions with metallurgy and the vendor regarding this condition did not yield a definitive cause. After vendor reassessment of his compliance with material process specifications and a material substitution to Steel Carbon Bar QQ-S-634 comp. 1018 Cold Finish, due to unavailability of additional quantities of Allegheny Ludlum Relay No. 5", a second rotor was fabricated satisfactorily.

4.1.3 Sub Assemblies

Difficulty was encountered in locating a qualified vendor to fabricate the servo valve mechanism. A shop considered suitable was eventually selected. Problems involving machining tolerances requiring a re-study and subsequent adjustment of the tolerance structure created a significant delay in the completion of this subassembly. Performance tests of the valve for air flow characteristics were conducted at Bendix due to the lack of proper test facilities at the vendor site.

4.2 ASSEMBLY

Assembly of the actuator required no specialized techniques or tooling. Only one minor problem occurred during initial assembly concerning the fit of the manifold plates to the stator assembly and is discussed in detail in the following sections. A parts list of the actuator is included in Appendix A for reference purposes.

4.2.1 Procedure

Final assembly of the actuator commenced with the stator assembly shown in Figure 4. This vendor fabricated unit consisting of stator laminations, pole coils, and vane blocks is the main structure of the actuator. The left manifold plate assembly, shown in Figure 5 prior to cementing the pneumatic transfer and manifold plates together, was assembled to the stator. A neoprene rubber gasket provides the proper sealing between the stator and manifold plate. The fixed output end gear, precisely positioned by a dowel pin and pilot hole arrangement was assembled to the manifold plate. The ring gear and roller bearings (Figure 6) were next assembled to the rotor (Figure 7). The rotor assembly, vanes, and output shaft were then slipped into place. Figure 8 is a photo illustrating the major internal components of the actuator. All gearing was coated with a molybdenum disulphide base lubricant, Bendix E.P. Lube Compound No. 1700-15.

The right manifold plate (Figure 9) was then installed followed by insertion of orbit shafts at eight places. Retaining rings hold the orbit shafts in position. Assembly of the fixed output end gear to the right manifold plate essentially completes the rotary motor portion of the actuator. Shimming between the end gears and manifold plates provides an adjustment for setting the output shaft end shake.

Attachment of the servo valve assembly, angular position sensor, crank arm and stops completed the final assembly of the actuator.

4.2.2 Problems

Dimensional measurement after initial assembly of the manifold plates to the stator indicated that the plates were not properly seated. A neoprene rubber gasket is utilized to form a seal between the manifold plates and the stator. Metal to metal seating between bosses on the plates and vane blocks on the stator establishes the amount of gasket compression. Nominally, the gasket is compressed .010 inches from a free thickness of .062 inches. Inspection after removal of the manifold plates revealed the existence of



STATOR ASSEMBLY

FIGURE 4



LEFT MANIFOLD PLATE - LEFT
PNEUMATIC TRANSFER PLATE

FIGURE 5

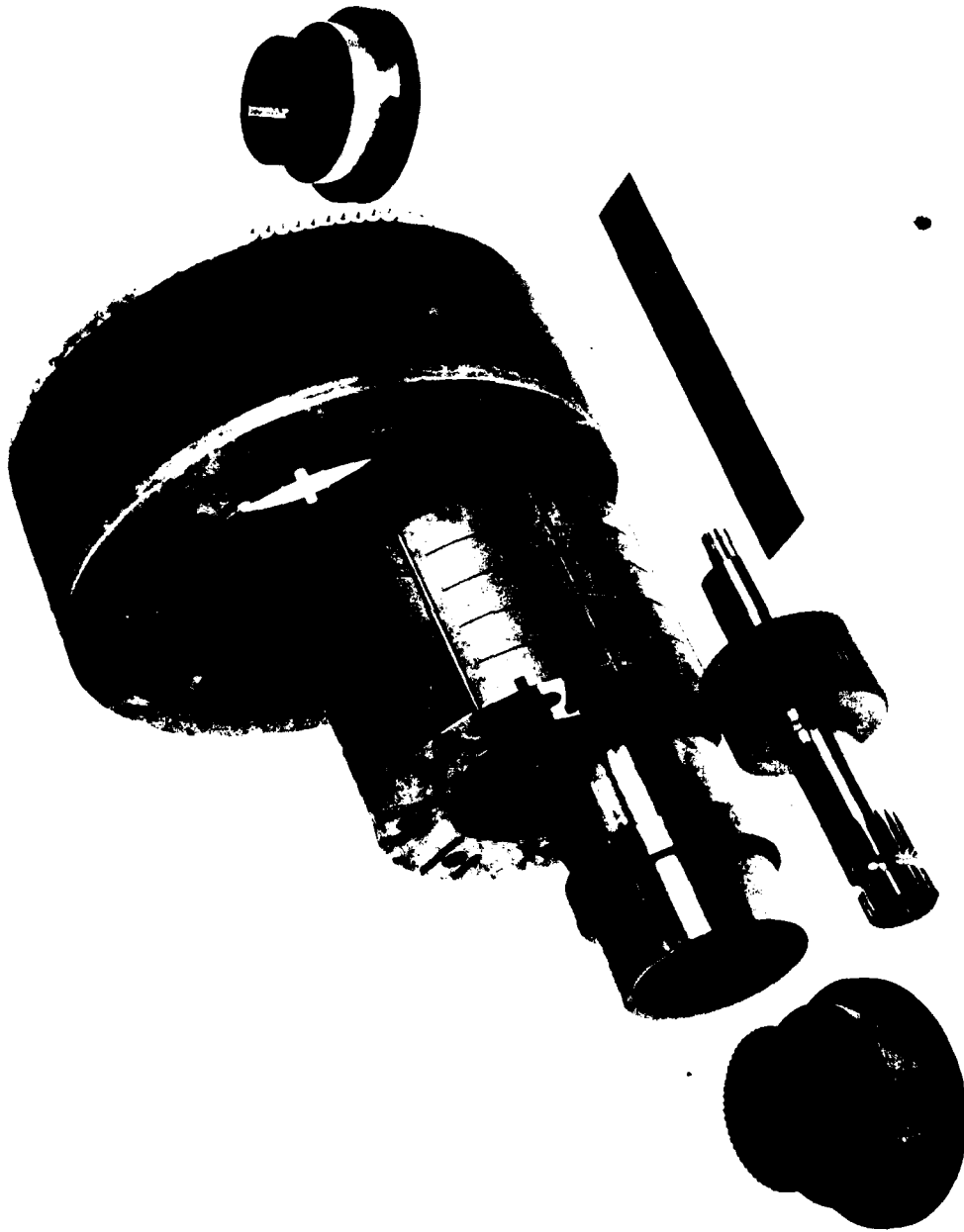


ROLLER BEARINGS - RING GEAR

FIGURE 6



ROTOR
FIGURE 7



GLARS - ROTOR - STATOR ASSEMBLY

FIGURE 3



RIGHT MANIFOLD PLATE - RIGHT
PNEUMATIC TRANSFER PLATE

FIGURE 9

interference areas created by excessive bulk in the stator coil windings, causing gasket over compression. As a result the metal to metal seating arrangement could not be achieved.

Rework of the gasket by enlarging gasket growth relief holes sufficiently to encompass the interference area appeared to have corrected the problem. However, air leakage flow and rotor clearance measurements made after re-assembly of the actuator indicated that the manifold plate misfit persisted.

The actuator was disassembled. Further inspection uncovered additional interference areas. Several stator coil windings exceeded the specified outline sufficiently to allow contact to occur with the manifold plates. Also, the stator overall width measured at the spacer rings was sufficiently high to cause excessive compression of the gasket in the spacer area. Relief areas were milled in the manifold plates to eliminate contact with the stator coil windings. The overall stator width was reduced by milling the spacer rings to allow for a nominal gasket fit. Measurements after reassembly of the actuator confirmed that both manifold plates were seated properly.

4.3 TEST METHODS AND RESULTS

The actuator was altered slightly from the flight test oriented configuration in order to allow the flexibility and monitoring required to conduct limited performance verification tests and demonstrations. Figure 10 is a hook-up drawing of the actuator test configuration and depicts the removal of the mechanical stops, substitution of the 360° RVDT in place of the 40° dual element RVDT, removal of the crank arm (except for torque tests), and installation of a test harness.

4.3.1 Pneumatic Mode

4.3.1.1 Servo Valve Mechanism

Tests were conducted on the servo valve mechanism to establish air flow characteristics and evaluate its suitability with respect to design criteria. The valve was mechanically connected to a micro-positioner, a device adapted

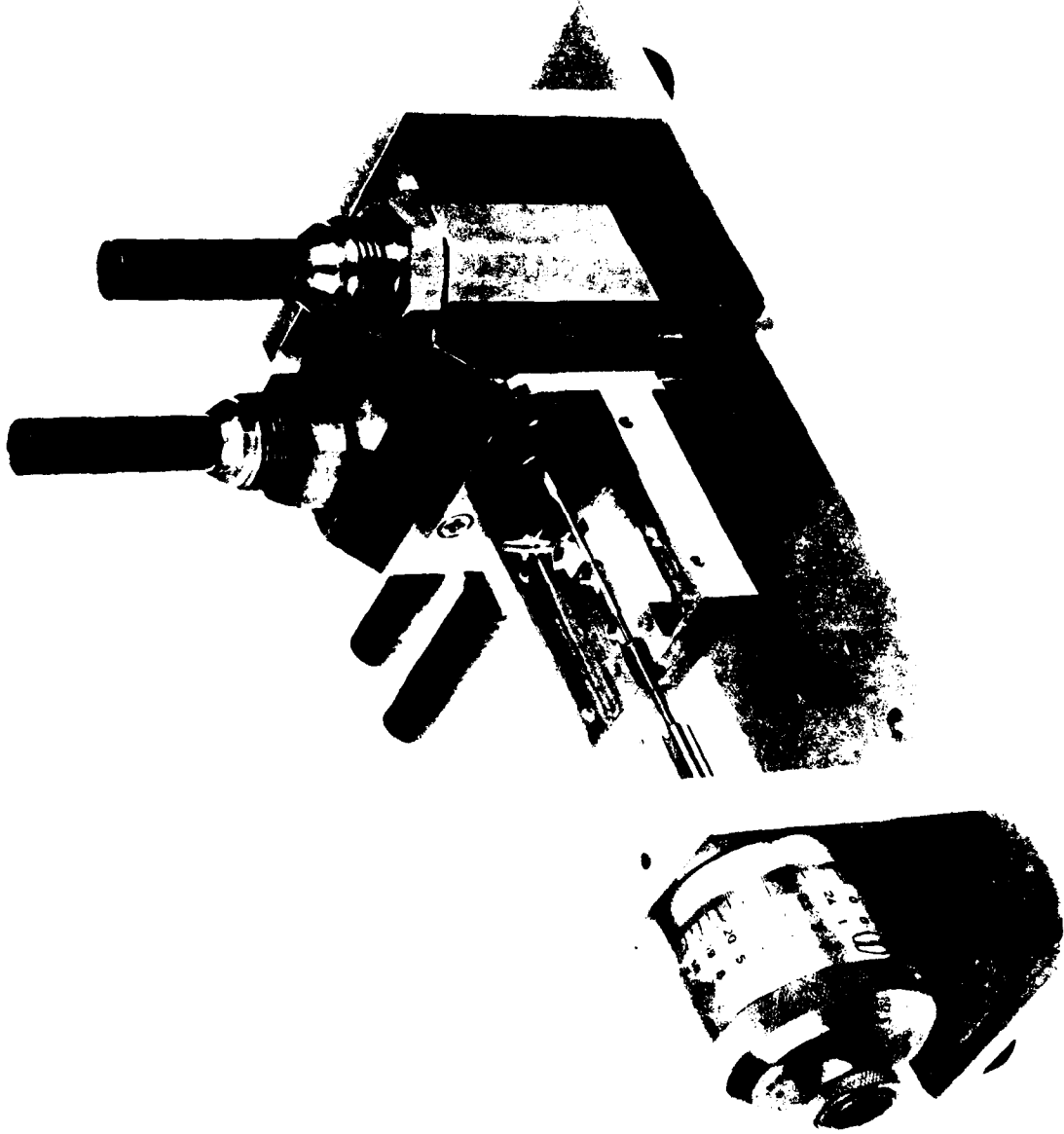
to precisely position and displace the valve spool. Linear displacement resolution of the micro-positioner was .0001 inch. Figure 11 is a photo of the valve mounted to the micro-positioner test fixture.

The valve was then pneumatically connected to a pressure source, flow-meter, and appropriate pressure gauges as shown in Figure 12. With the supply pressure set at a regulated 20 psig, flow measurements were obtained from 0 (Null) to .015 inch valve spool displacement on either side of null in .001 inch increments. Figure 13 is a plot of air flow vs. valve travel and compares the results to design criteria. An excessive deadband at null indicates a valve underlap. Rework of the valve to improve null sensitivity would correct air flow gain to within specified limits. However, the valve exhibited adequate capacity to supply rated and maximum air flow levels. Also, initial test results of the actuator motor indicated that the measured valve air flow characteristics would not detract from expected actuator performance. Rework of the valve was therefore deferred.

4.3.1.2 Actuator

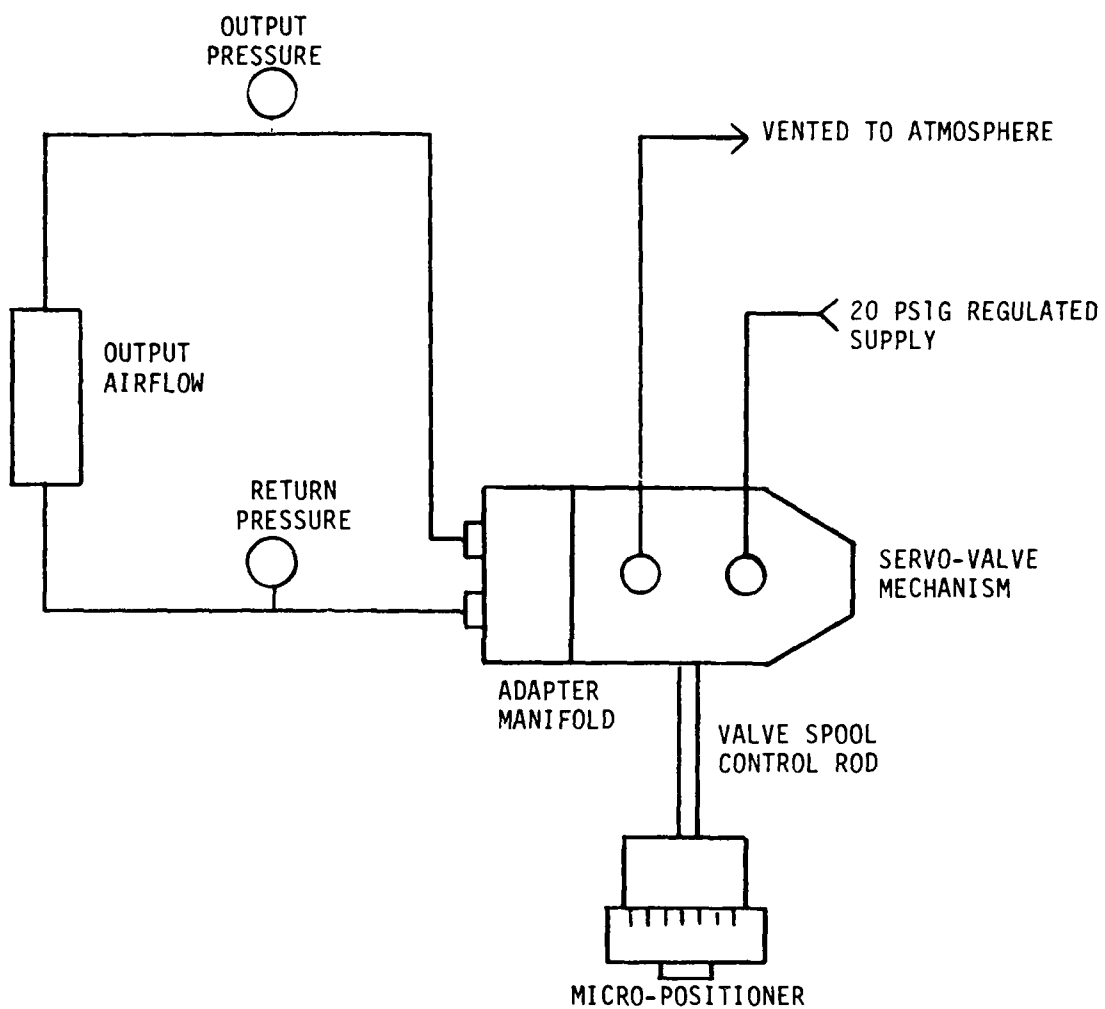
Tests were conducted to insure pneumatic integrity of the actuator and establish its basic performance capabilities. The servo valve was by-passed during initial tests in order to focus attention on the actuator motor alone. In subsequent tests, operation and directional control were established with the servo valve installed and an open-loop command signal applied to the servo valve torque motor.

For test purposes the actuator was affixed to a shock mounted holding fixture. The output shaft was positioned horizontally. Input and return pneumatic connections to the actuator were made through an adapter manifold. Input pressure was controlled by a standard diaphragm type regulator. Flow-meters and pressure gauges were interconnected in the test circuit in order to monitor and record pertinent air flow and pressure levels. Figures 14 and 15 are photos of the test installation. Figure 16 is a diagram of the bench test set-up.



SERVO VALVE FLOW TRIM TEST FIXTURE

FIGURE 11



SERVO VALVE MECHANISM AIRFLOW TEST DIAGRAM

FIGURE 12

EUGENE DIEZGEN CO.
MADE IN U.S.A.

DIEZGEN GRAPH PAPER
MADE IN U.S.A.

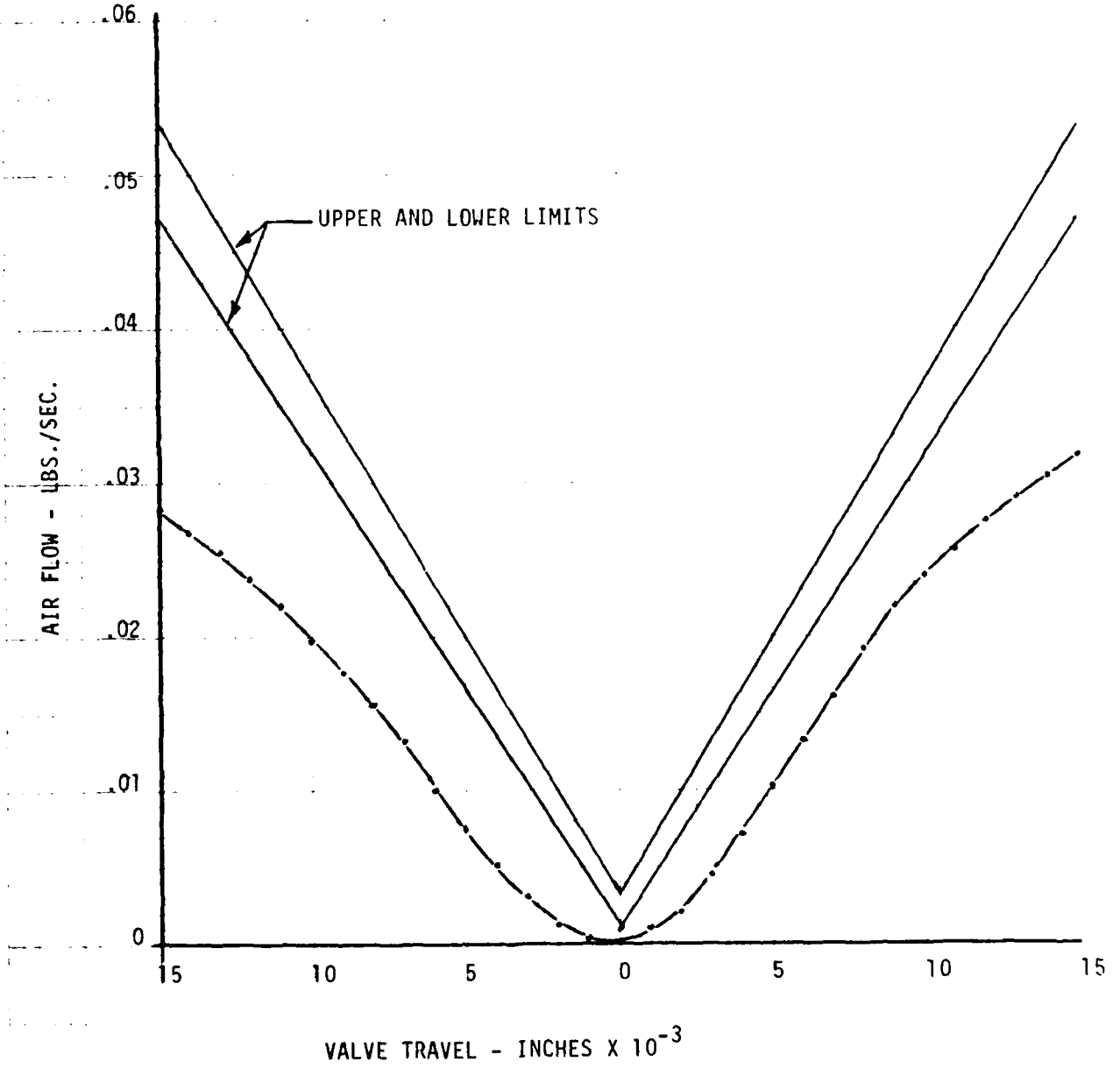
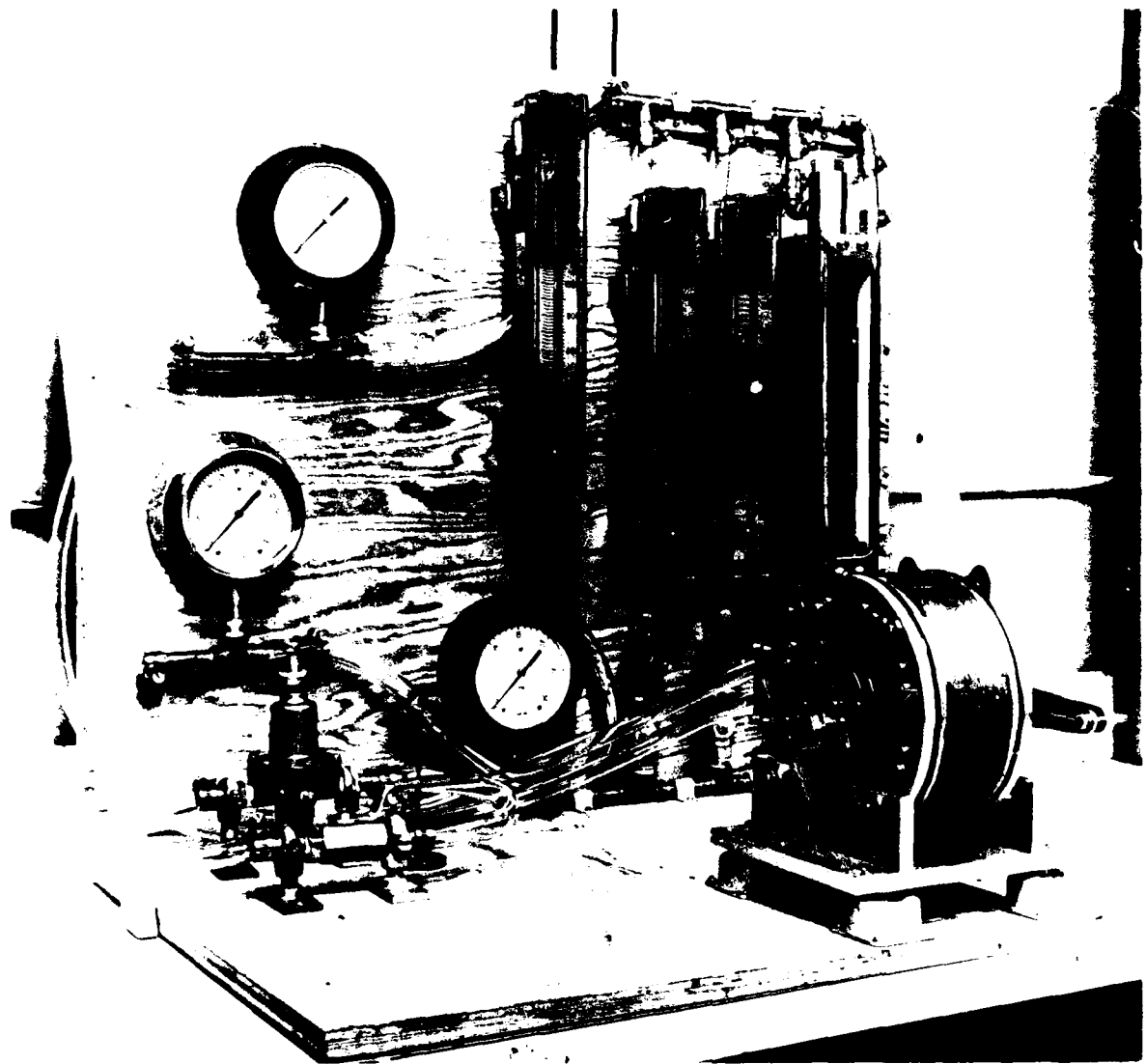


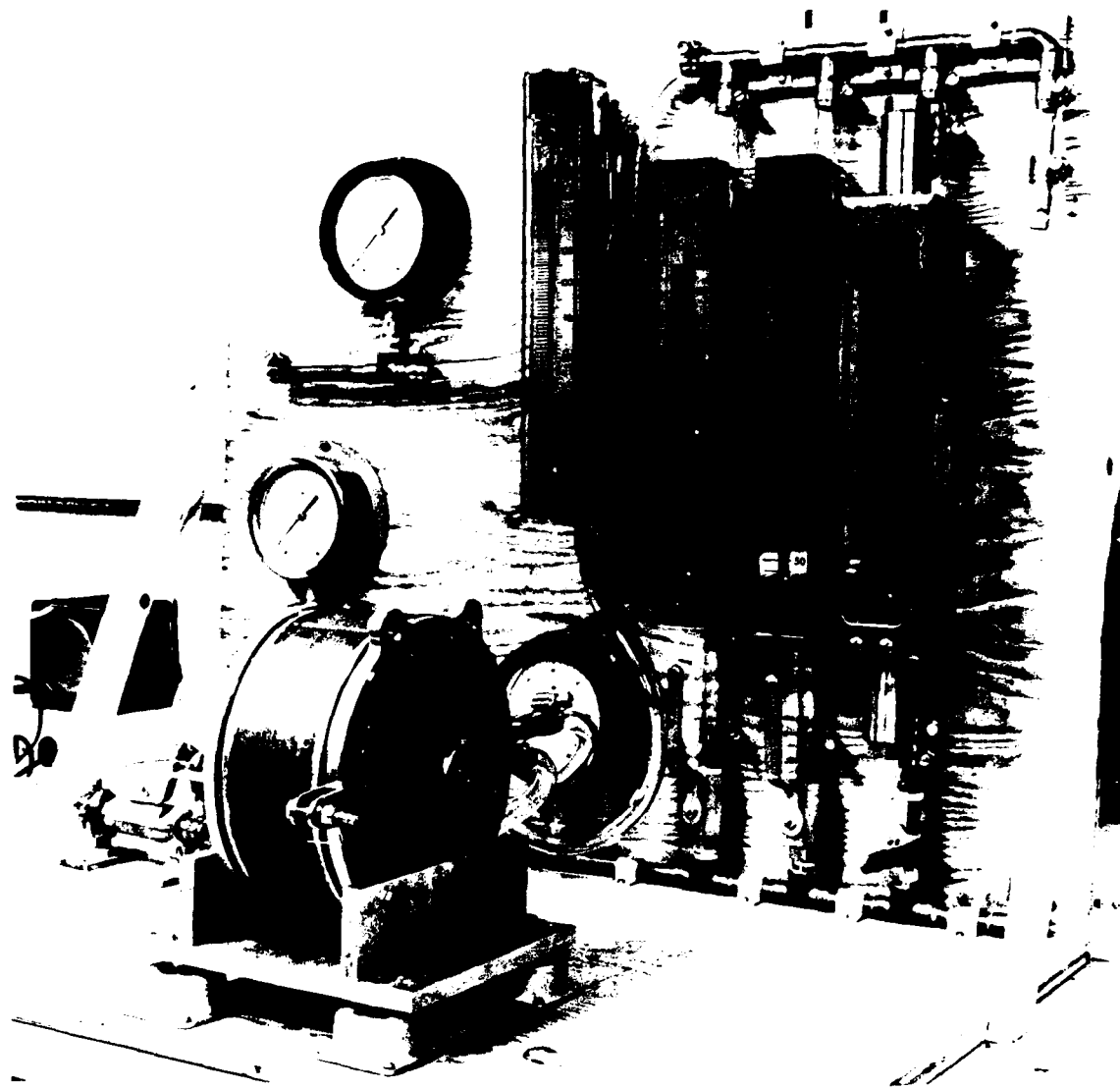
FIGURE 13 - SERVO VALVE MECHANISM AIR FLOW

FIGURE 13



PNEUMATIC MODE TEST SET-UP
ELECTRO-PNEUMATIC ACTUATOR

FIGURE 14



PNEUMATIC MODE TEST SET-UP
ELECTRO-PNEUMATIC ACTUATOR

FIGURE 15

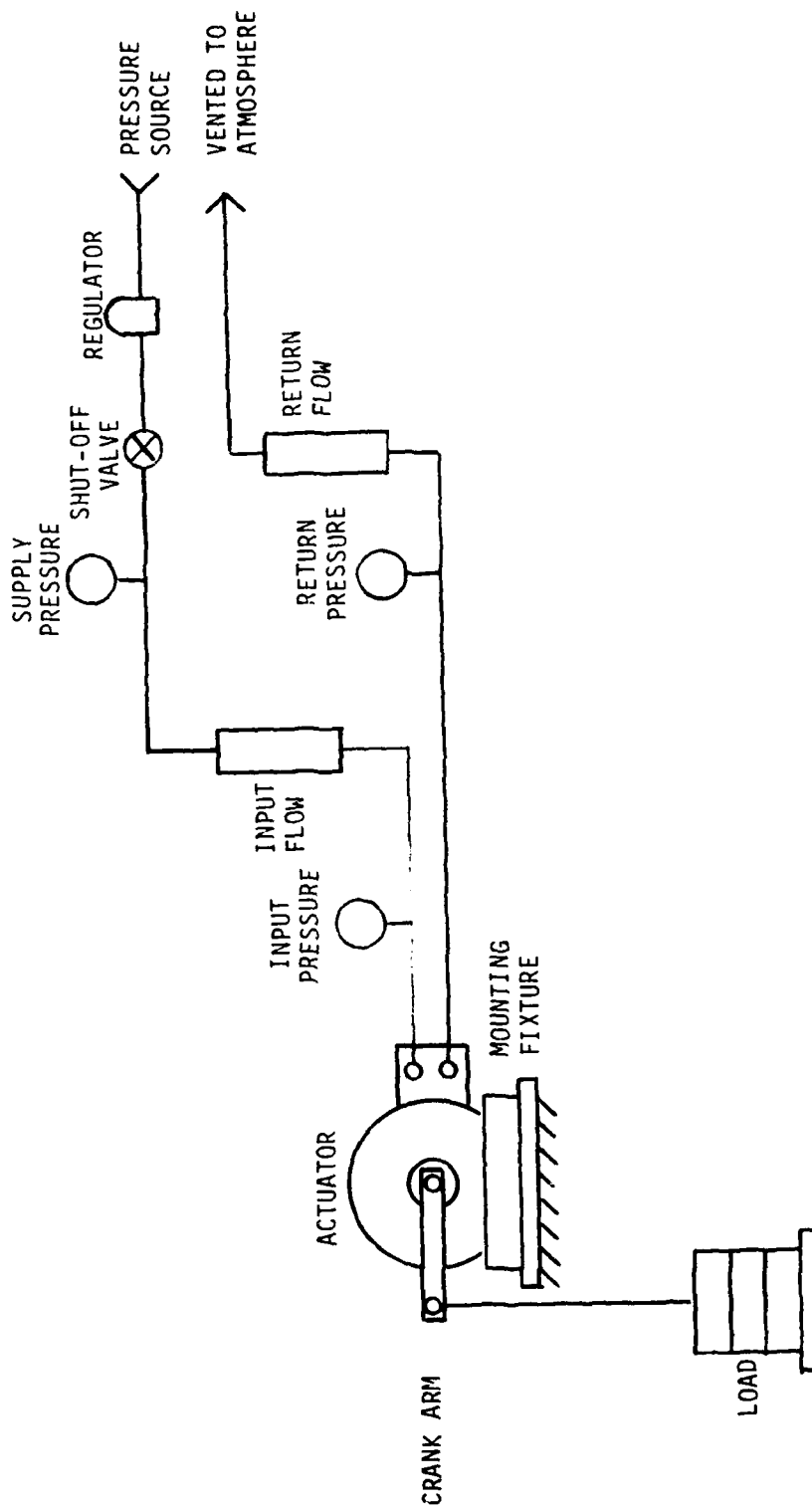


FIGURE 16 - ELECTRO/PNEUMATIC ACTUATOR PNEUMATIC MODE OPEN LOOP TEST DIAGRAM

4.3.1.2.1 Flow Losses

Cross port and case leakage create flow losses which, if significantly high, can result in power loss. These flow losses are determined by measuring input and return air flow. With 20 psig applied to the actuator input port and the return port vented to the atmosphere, input and return air flows were recorded. The actuator was maintained in a stalled condition by applying sufficient back torque to the output shaft. Computation of the flow losses are described below.

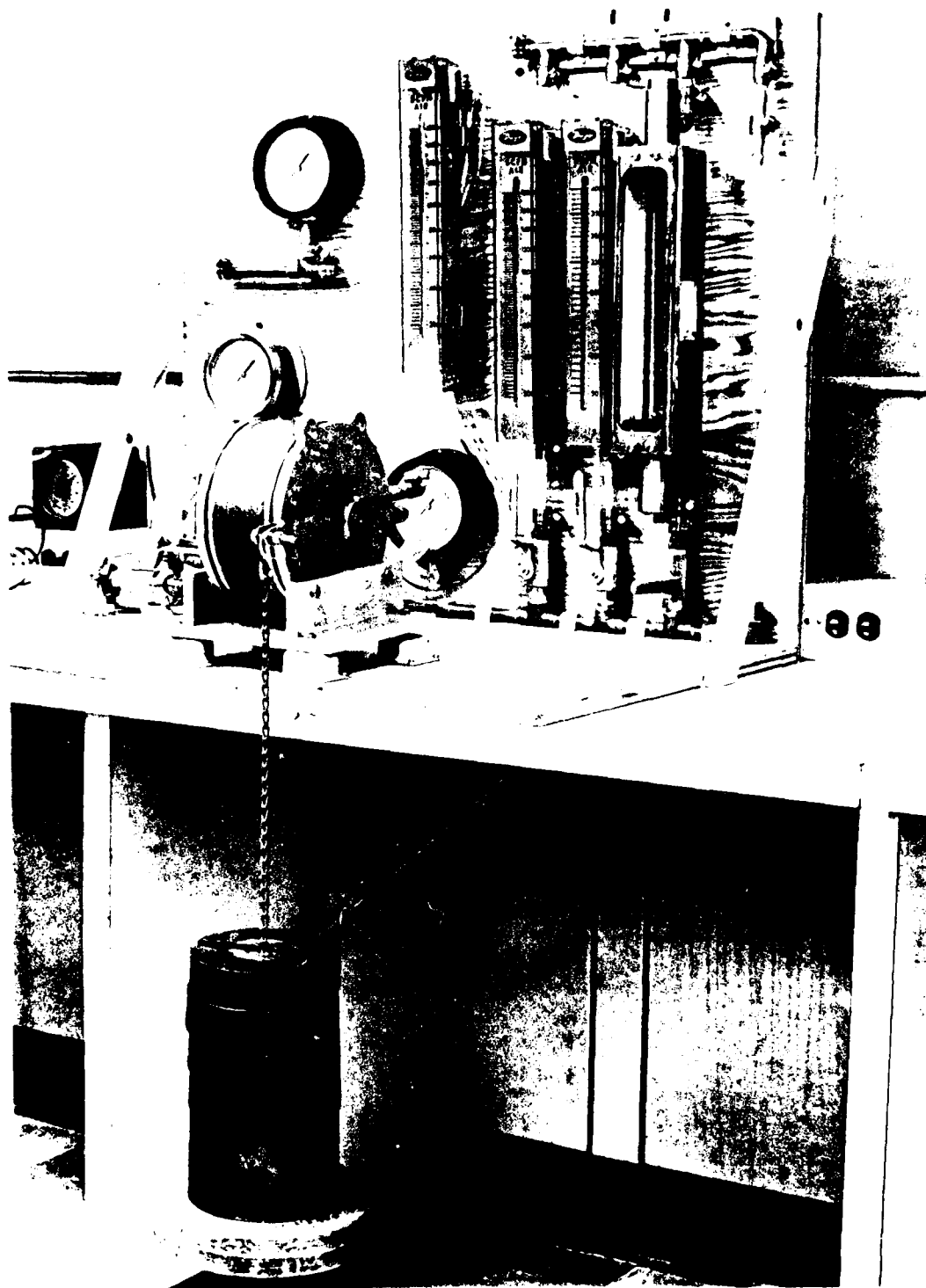
$$\begin{aligned} \text{Case Leakage Flow Loss} &= \text{Input Flow} - \text{Return Flow} \\ &= .0137 - .0129 = .009 \text{ lbs/sec.} \end{aligned}$$

$$\text{Cross Port Flow Loss} = \text{Return Flow} = .0129 \text{ lbs/sec.}$$

Case leakage flow loss (.0009 lbs/sec) is relatively low and consistent with leakage expected where gasket, "O" ring, and bearing seals are employed. Cross port leakage flow loss (.0129 lbs/sec) is within the predicted value (.0134 lbs/sec) computed from leakage paths created by nominal mechanical clearances. Total measured flow loss (.0138 lbs/sec) would therefore not compromise actuator performance.

4.3.1.2.2 Torque/Speed

Basic performance of the actuator in the pneumatic mode can best be established by determining its torque/speed characteristics. Accordingly, bench tests were conducted with the actuator operating under varying torque loads during which speed measurements were obtained. The horizontal attitude of the actuator output shaft facilitated application of torque by loading the crank arm with weights as illustrated in Figure 17. Angular shaft speed was determined by timing the motion of the crank arm over an arc from 9° below horizontal to 9° above horizontal. The error encountered in actual applied torque due to this swing through an arc, calculated to be 1%, was considered insignificant and therefore not taken into account in the torque measurements. Input pressure to the actuator was maintained at 20 psig during these tests.



PNEUMATIC MODE TORQUE TEST SET-UP
ELECTRO/PNEUMATIC ACTUATOR

FIGURE 17

Figure 18 is a plot of the recorded torque/speed test data and compares the results with design goals. Measured no load speed was within 60% and stall torque within 30% of predicted values. The actuator was re-positioned to place the output shaft in a vertical attitude with no affect noted in no load speed performance. Stall torque measurements were not obtained due to the difficulty in applying torque load in this attitude. However, absence of any affect on the no load speed with actuator attitude change indicates that torque performance would be similiary unaffected.

4.3.2 Electric Mode

4.3.2.1 Insulation Resistance

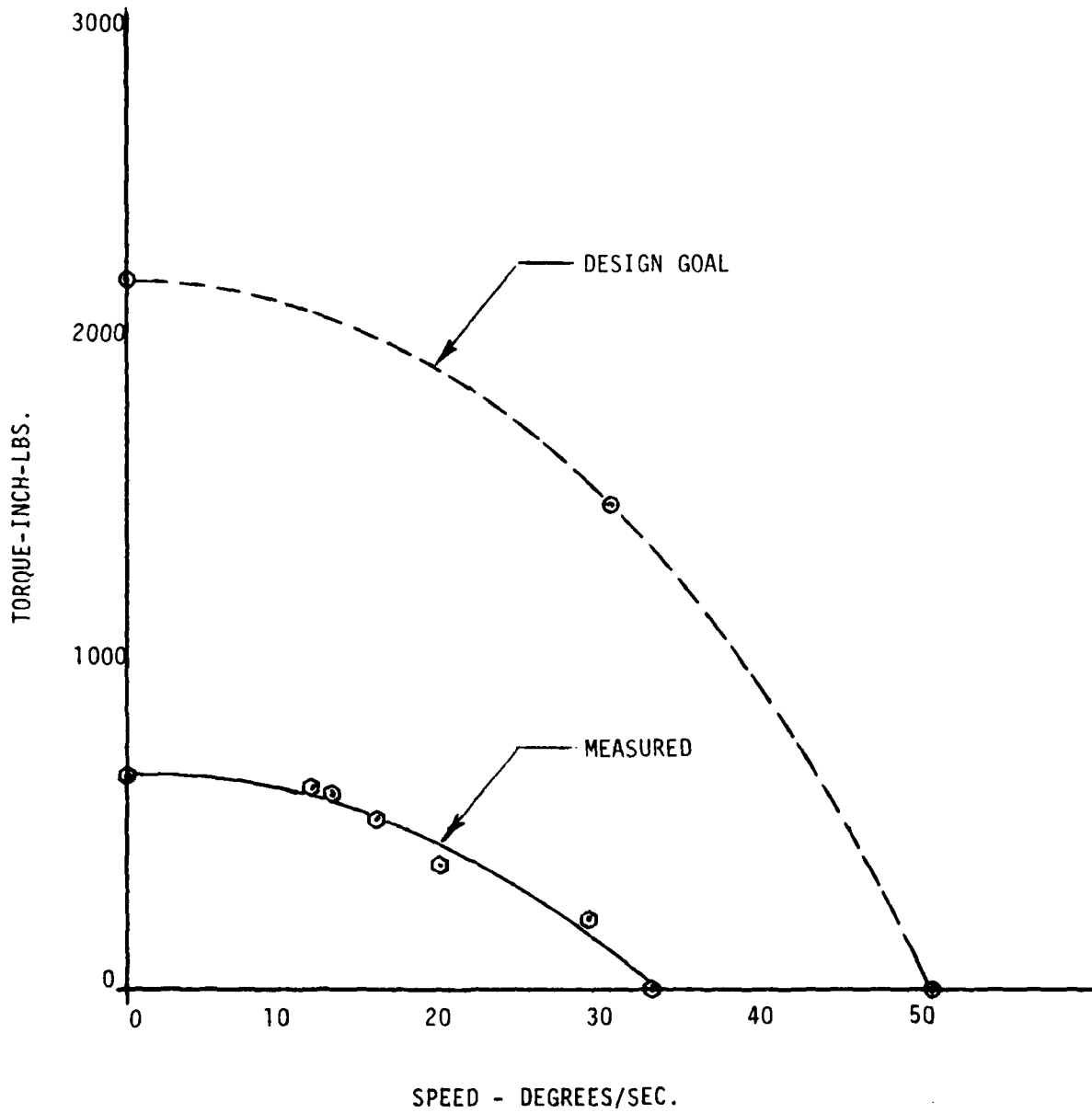
200VDC was applied between the common of each set of 4 stator coils and the actuator case. No insulation breakdown was observed. Leakage current was determined to be insignificant.

4.3.2.2 Torque/Speed

Open loop tests were conducted on the actuator in the electric mode with a breadboard power drive providing coil excitation sequencing and power. Figure 19 is a photo of the bench test set-up. Figure 20 illustrates the test connections. Preliminary tests showed that actuator stall would occur when coil excitation was increased above 80 volts. The following tests were conducted, therefore, at approximately 75 volts.

The maximum no load speed attainable was 19.8°/sec. Increasing the coil sequencing rate resulted in actuator stall.

Maximum stall torque could not be determined due to the limited torque load available from the load fixture. However, an approach to stall condition was developed by applying the maximum torque load of 686 inch lbs. and increasing the coil sequencing rate until a stall developed. This occured at an equivalent speed of 8.8°/sec.



ELECTRO/PNEUMATIC ACTUATOR PNEUMATIC MODE TORQUE-SPEED CURVE

FIGURE 18

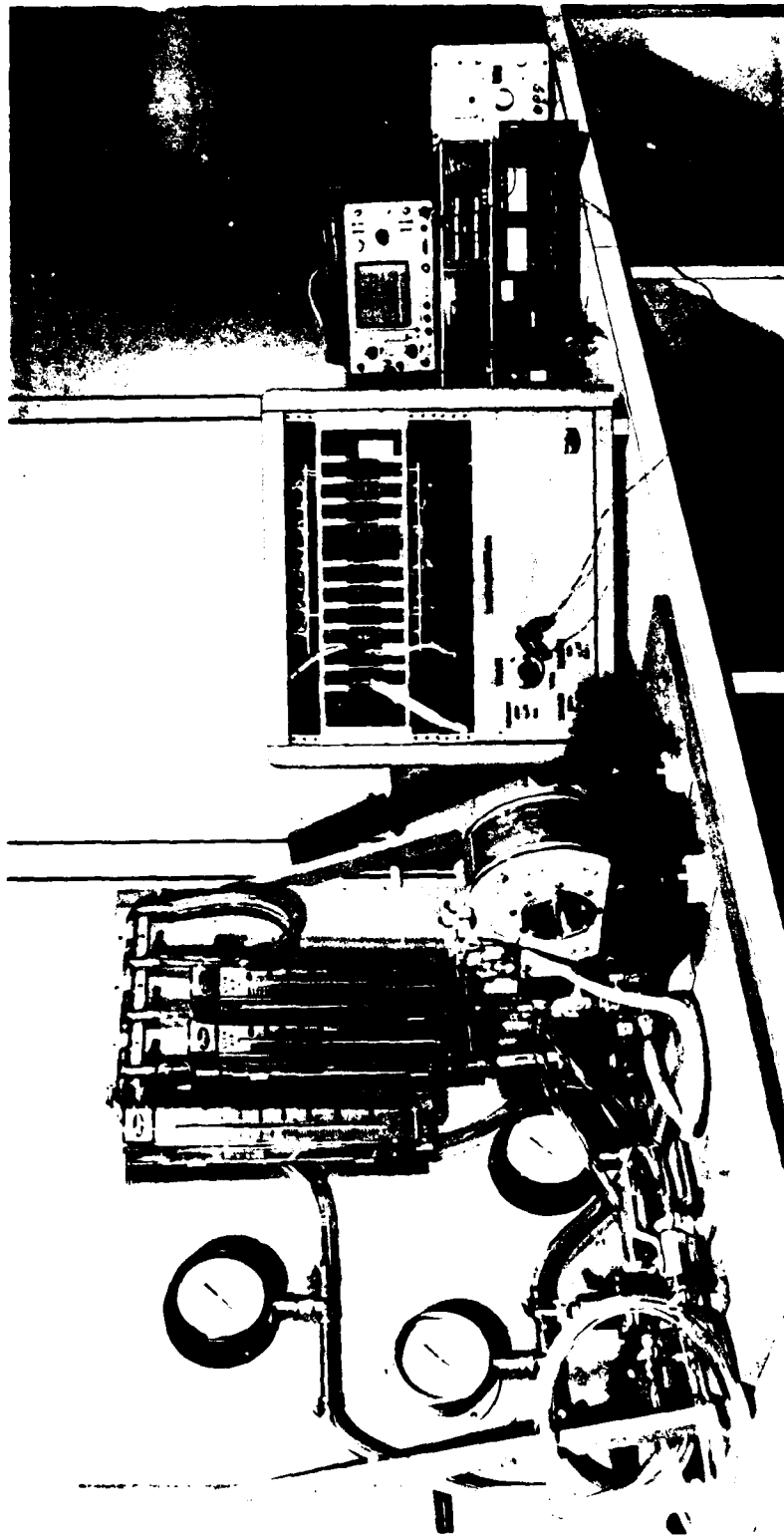


FIGURE 10 PNEUMATIC AND ELECTRIC MODE OPEN LOOP TEST SET-UP

FIGURE 19

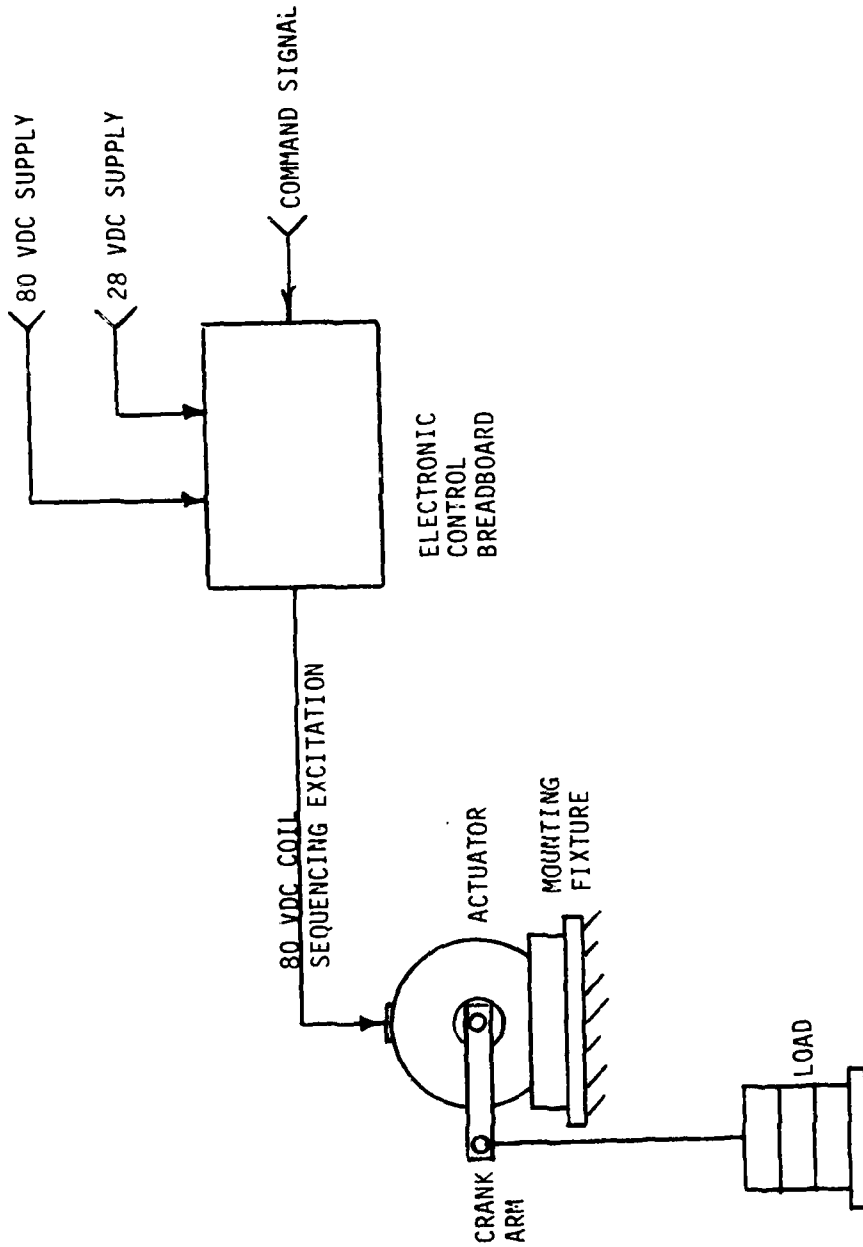


FIGURE 20 - ELECTRO/PNEUMATIC ACTUATOR ELECTRIC MODE OPEN LOOP TEST DIAGRAM

Figure 21 is a plot of the data points and compares the results with design goals.

4.3.2.3 Power Consumption

Actuator power consumption during no load, open loop operation was measured at 5 amps at 80 VDC.

4.3.3 Transient Response

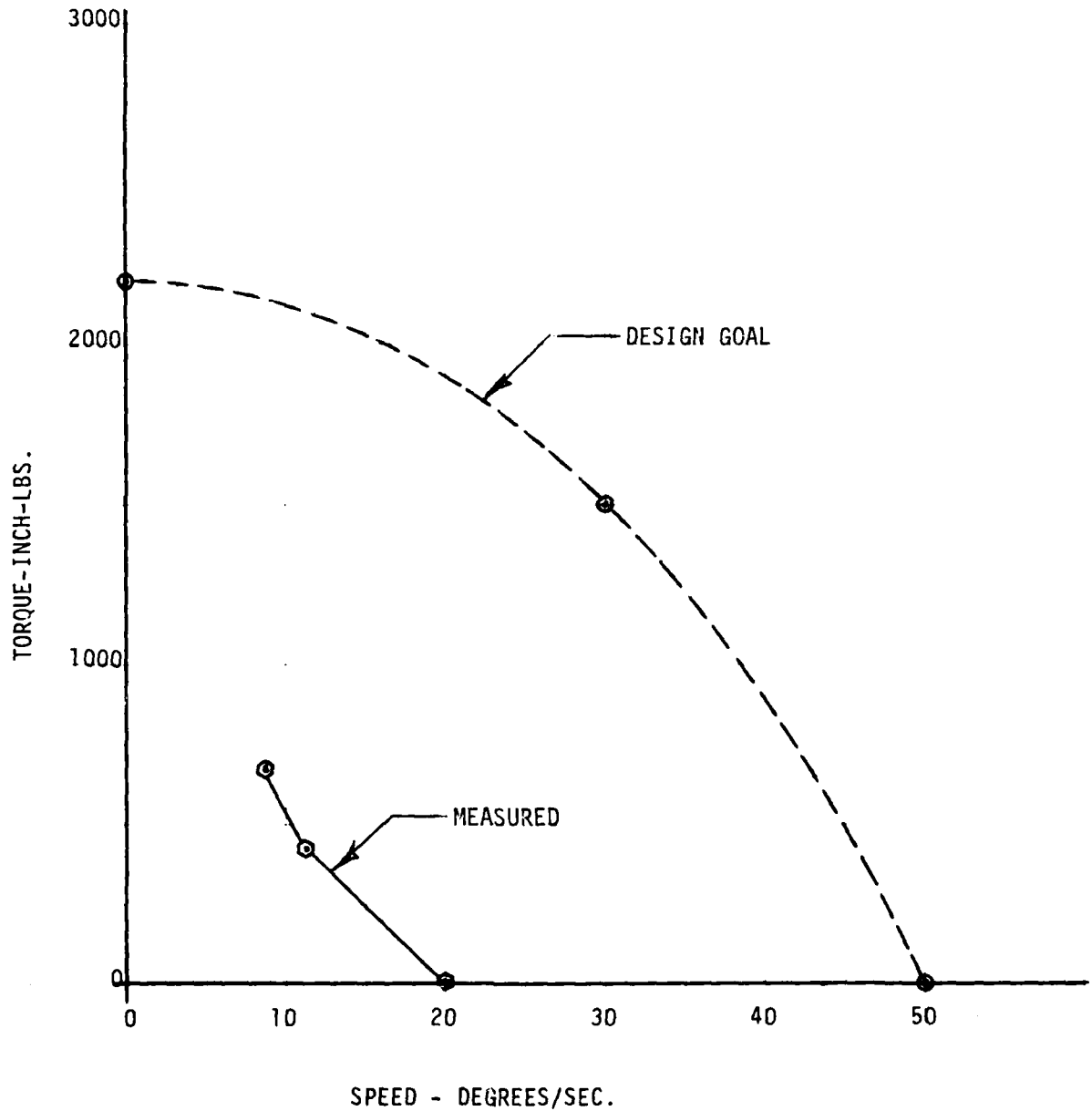
Open loop transient response tests were conducted to obtain a first indication of the actuators dynamic behavior. The tests were performed in both the pneumatic and electric modes under a no-load condition. The recorded output from an RVDT mounted to the actuator output shaft was used to monitor the actuator response. Transient input stimuli to the actuator were generated by introducing discreet input command signals through an on-off switch.

Figure 22 is a photo of the bench test set-up. Figure 23 is a diagram of the equipment interconnections. Actuator response to various step input signal levels were obtained. Figures 24 through 26 are strip recordings of the command signal input and actuator shaft position sensor output signals. Maximum response time for stabilization was determined to be 60 milliseconds.

4.4 TEARDOWN INSPECTION

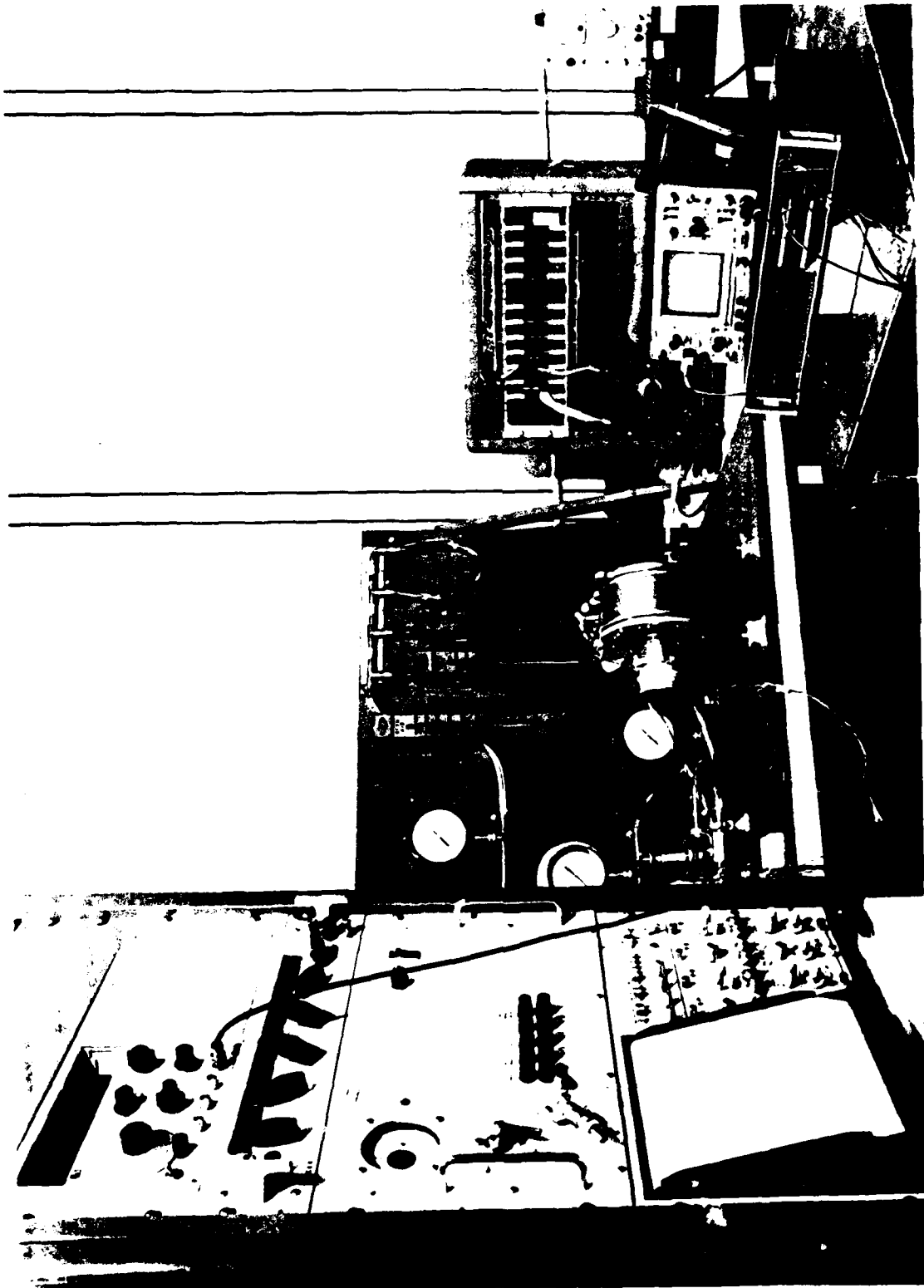
The actuator was disassembled after accumulating approximately 8 hours of operation. Internal components were examined for evidence of excessive wear.

The orbit shafts showed excessive wear patterns in the area of contact with the rotor. The wear condition was determined to be fretting corrosion caused by high bearing loads. The shafts were intended to operate without lubrication in initial design considerations where a hardened, chrome plated surface was considered adequate for the anticipated bearing load. A dry lubricant similar to that used on the pneumatic transfer plates, was applied to the orbit shafts and appeared to have retarded the progression of the fretting corrosion in subsequent teardown inspections. A more permanent design



ELECTRO/PNEUMATIC ACTUATOR ELECTRIC MODE TORQUE-SPEED CURVE

FIGURE 21



"PNEUMATIC AND ELECTRIC MODE OPEN LOOP
TRANSIENT RESPONSE TEST SET-UP"

FIGURE 22

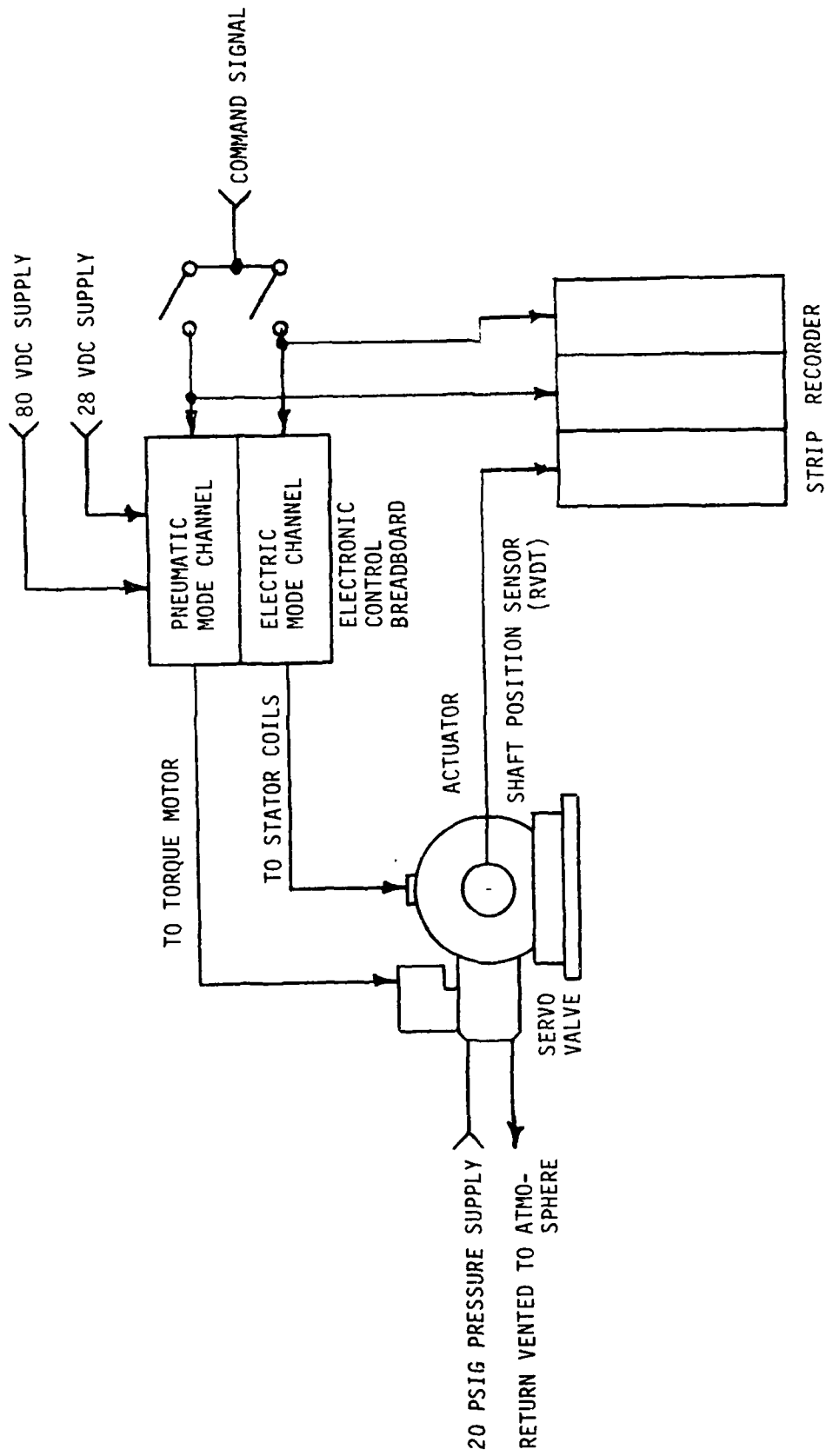


FIGURE 23 - ELECTRO/PNEUMATIC ACTUATOR OPEN LOOP TRANSIENT RESPONSE TEST DIAGRAM

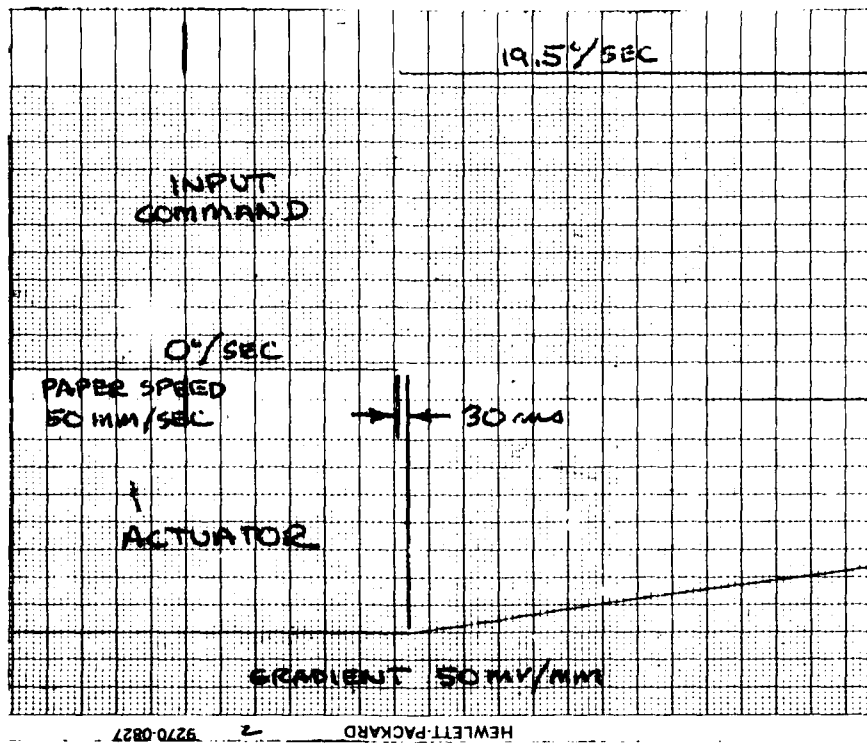
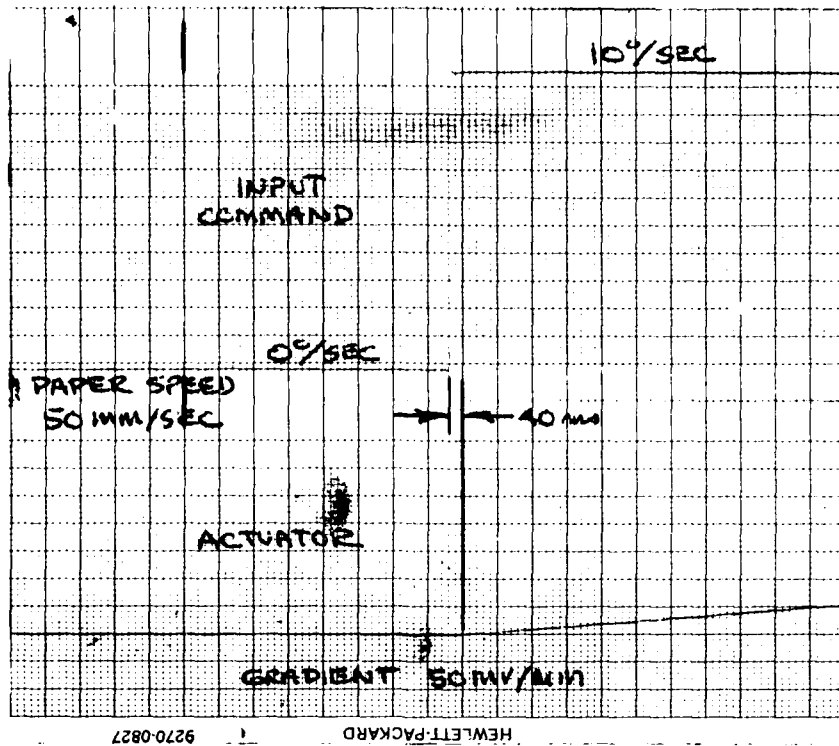


FIGURE 24 - ELECTRO/PNEUMATIC ACTUATOR PNEUMATIC MODE OPEN LOOP TRANSIENT RESPONSE

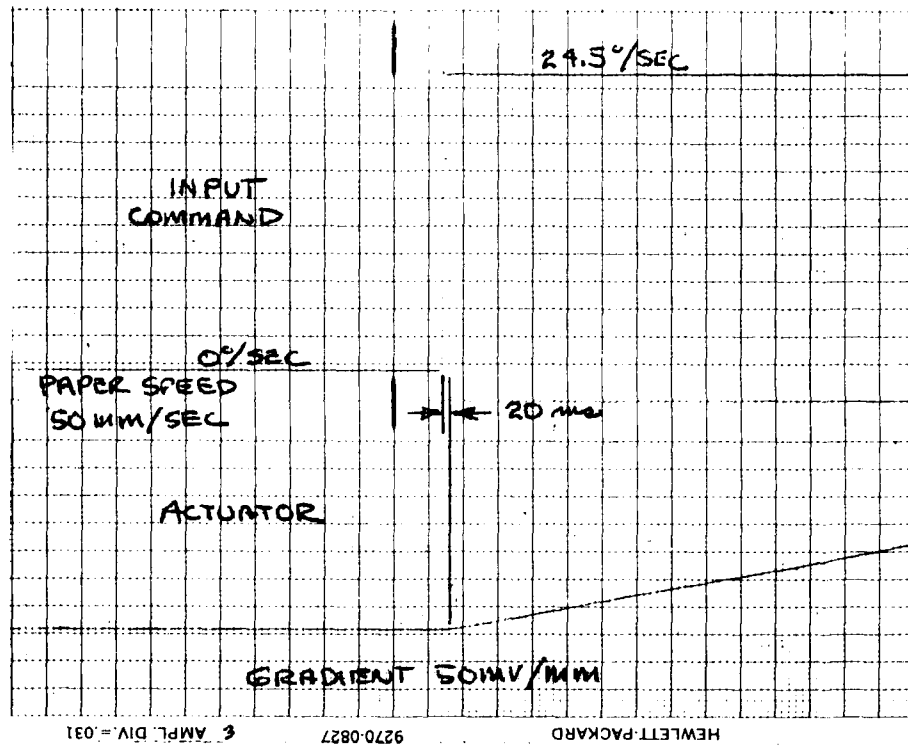


FIGURE 25 - ELECTRO/PNEUMATIC ACTUATOR PNEUMATIC MODE OPEN LOOP
TRANSIENT RESPONSE

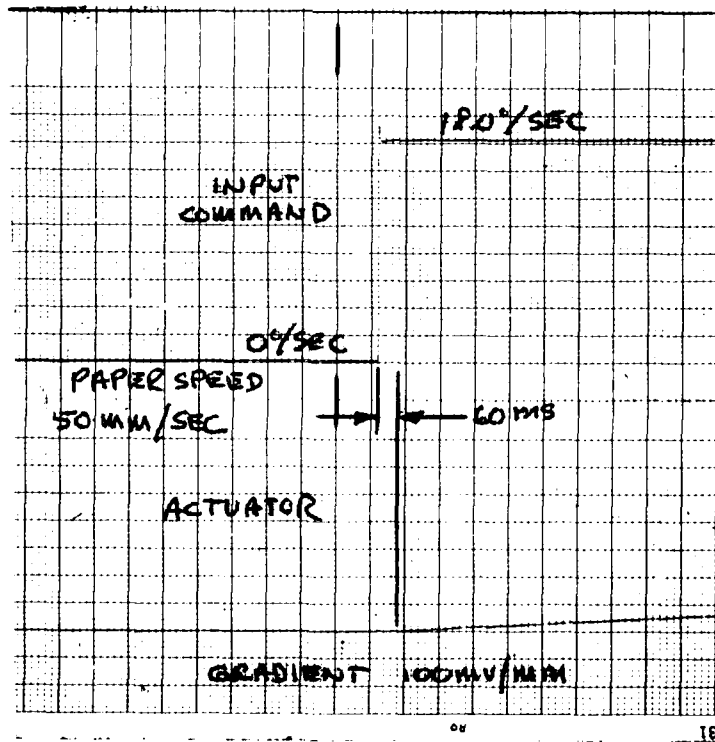
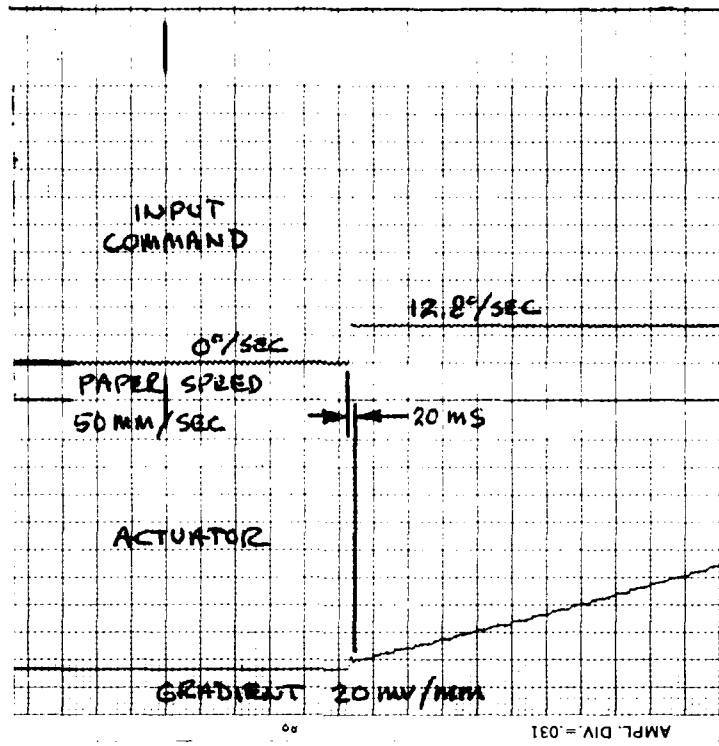


FIGURE 26 - ELECTRO/PNEUMATIC ELECTRIC MODE OPEN LOOP
TRANSIENT RESPONSE

fix may be required such as increasing the orbit shaft diameter to decrease the bearing load.

No other indications of abnormal wear in the remaining internal components were noted.

4.5 PERFORMANCE ANALYSIS

In testing of the dual mode actuator, in the electric mode, when the voltage was increased much above 75 volts, partial separation of the gears occurred. Interference of the gear teeth prevented complete separation, but resulted in stalling the actuator. In the pneumatic mode partial separation occurred, which resulted in decreasing the torque output. It did not stall the actuator.

The dual mode actuator gearing configuration was based on the previous designs of a series of successful pneumatic and electric actuators using epicyclic gearing. In these actuators the ring gear had no support bearing. As in any gear mesh, a component of the force acting on the gear teeth is in the direction to cause gear separation. The gear separation force is given by

$$F_S = \frac{1}{R_O} T \tan \theta \quad (1)$$

where

R_O = Output gear pitch radius, in

T = Output torque, in-lbs

θ = Gear tooth pressure angle

The output torque is

$$T = e R_q F_r \cos \phi \quad (2)$$

where

e = eccentricity

R_q = Gear ratio

F_r = Force applied to rotor

ϕ = Rotor force vector angle

Substituting for T in equation (1) gives

$$F_s = \frac{e}{R_o} R_q F_r \tan \theta \cos \phi$$

Thus, for a given force F_r , the separation force increases as the gear ratio is increased.

For the pneumatic actuators the commutation angle was selected so that a component of the pneumatic force applied to the rotor was in the direction to cancel the separation force. This prevented gear separation.

Prior electric actuators operated on 28 volts. These actuators have a variable air gap. The magnetic flux density varies inversely with the gap according to the equation

$$B = 0.4 \pi \frac{NI}{g}$$

where

B = Flux density, gauss

NI = Ampere turns excitation

g = Gap length, cm.

The force is proportional to the flux density squared

$$F_p = K B^2$$

Thus, the force is high at the poles with small gaps, and is lower at the poles with larger gaps. This effect causes the resultant vector to act in the direction to provide a component for cancelling the separation force. There were no separation problems with these actuators.

The dual mode actuator has a substantially higher gear ratio than the prior pneumatic actuators. This results in a higher ratio between the gear separation force and the pneumatic force applied to the rotor. Therefore, even though the force vector angle is the same as for the prior pneumatic actuators, the normal component is not great enough to cancel the gear separation force, and some separation occurs.

In the electric mode, at higher voltage, the force is increased at the poles with larger gaps. The force cannot increase at the poles with smaller gaps because the iron is magnetically saturated. This caused the normal component of the rotor force to be reduced so that the separation occurs. The following analysis illustrates this phenomenon.

Assume the 4 excited poles are at 22.5°, 67.5°, 112.5°, and 157.5°. The air gap lengths are then

$$g = c + e (1 - \cos \theta) = 0.0127 + 0.119 (1 - \cos \theta), \text{ cm}$$

$$g_1 = .0218$$

$$g_2 = .0862$$

$$g_3 = .1172$$

$$g_4 = .2416$$

The air gap flux density at each pole is given by

$$B = .4 \pi \frac{NI}{q} \text{ gauss}$$

N = Number of turns per coil

$$B = .4 \pi \times 450 \frac{I}{g} = 565 \frac{I}{g} \text{ (iron saturates at about 15,000 gauss)}$$

The force per pole is given by

$$F_p = K B^2$$

Thus, B^2 is proportional to the force. For 1.0 amp per coil, at the 4 poles

B	B^2
15,000	225×10^6
6,555	43×10^6
4,821	23×10^6
2,339	5×10^6

$$F_x/K = B^2 \sin \theta = 149 \times 10^6$$

$$F_y/k = B^2 \cos \theta = 210 \times 10^6$$

For 3 amps per coil

B	B^2
15,000	225×10^6
15,000	225×10^6
14,462	209×10^6
7,016	49×10^6

$$F_x/K = 317 \times 10^6$$

$$F_y/K = 168 \times 10^6$$

$$\text{Vector angle} = 28^\circ$$

Thus, increasing the coil current has the effect of reducing the force vector angle, and thus reducing the component which helps to prevent gear separation.

5.0 CONCLUSIONS AND RECOMMENDATIONS

The original objective of inclining the rotor force vector to eliminate the rotor bearings was to eliminate the friction loss in these bearings, and to reduce the number of components. This approach was satisfactory for actuators with low power output, and with low gear ratios. However, for the higher power

actuators, the amount of force required to maintain gear contact becomes excessive. The force used to maintain gear contact produces no output power, therefore, there is a reduction in output power.

In the future, actuators of this type should have the rotor supported by eccentric bearings. Figure 27 shows how the rotor of an electric epicyclic gear motor can be supported by two eccentric bearings. Each eccentric bearing consists of an inside set of rollers in contact with the housing, an outside set of rollers in contact with the rotor, and an eccentric ring separating the two sets of rollers. An additional roller bearing separates the ring gear from the rotor as shown in Figure 28.

The eccentric bearings and reaction pins constrain the rotor to move with orbiting motion so that the gears will always remain in contact. The bearing separating the ring gear from the rotor allows the ring gear to rotate.

Figure 28 also shows how the electromagnetic force can be produced in the tangential direction. Applying the force in the tangential direction results in a mechanical advantage which would result in a significant weight reduction.

Development of the foregoing design concepts are recommended for achieving a vast improvement in actuator performance and enhancing its suitability for rotary control applications.

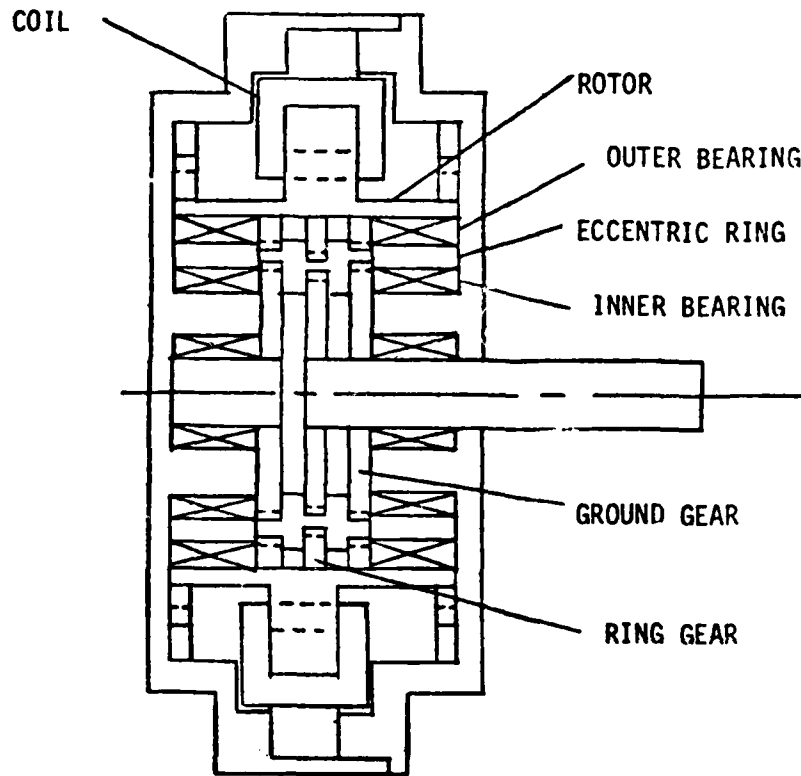


FIGURE 27 - 8 POLE HIGH RATIO ACTUATOR

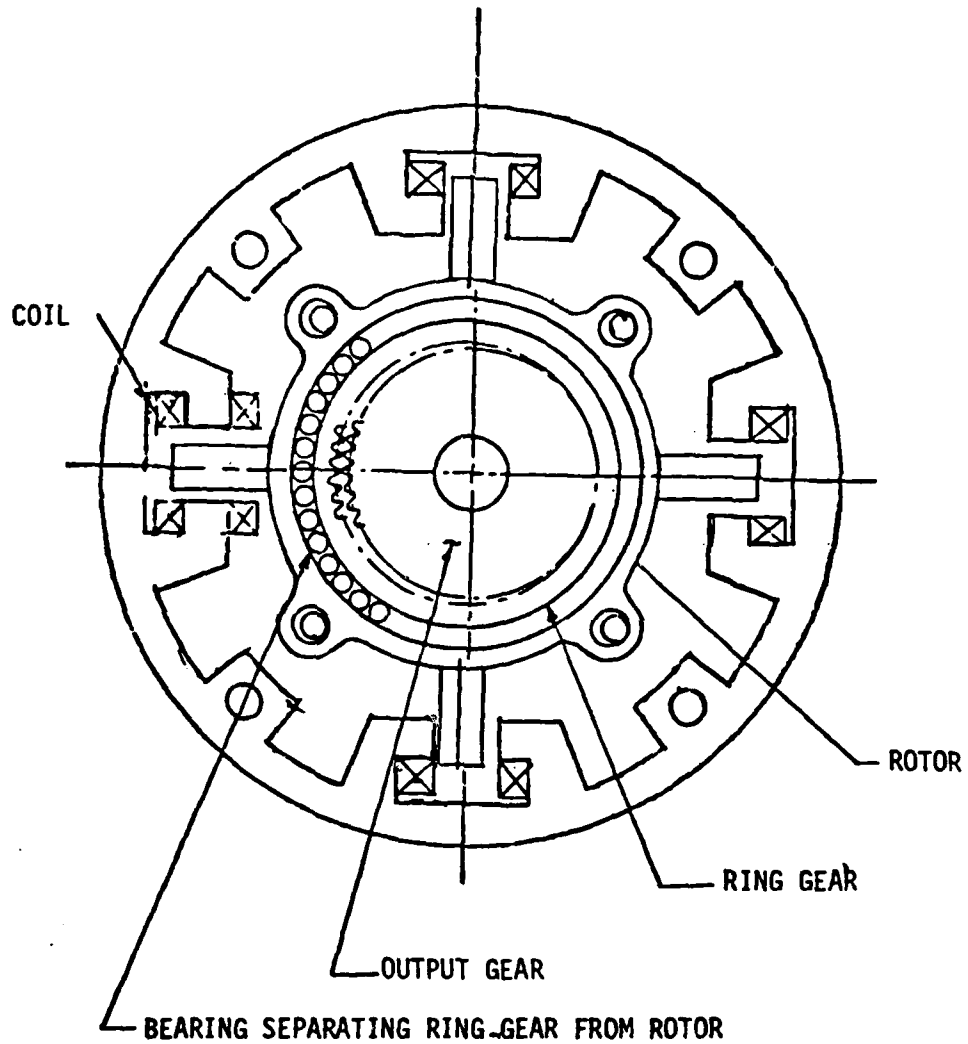


FIGURE 28 - 4 POLE HIGH RATIO ACTUATOR

NADC 82047-60

APPENDIX A

THE BENDIX CORPORATION NAVIGATION & CONTROL GROUP TETERBORO, N. J. 07608				19315		LIST NUMBER PL 3854020-1											
REMARKS:				CODE IDENT SHEET NUMBER 2		PREP: MENDILE 14-178											
				CKD:													
IT. REV.	ITEM NO	#=NEW	REV	B	QTY REQ	SIZE	PART NO.	FIND NO.	VENDOR PART NO.	ASSEMBLY LEVEL						DESCRIPTION	REL NO.
										1	2	3	4	5	6		
	1	#	1	F			3854020-1			ELECTRO-PNEUMATIC ACTUATOR, DUPL MODE							
	2																
	3																
	4																
	5	#	1	D			2797456-1			STATOR ASSEMBLY							
	6																
	7	#	1	C			2797457-1			SPACER, RIGHT							
	8	#	1	C			2797458-1			SPACER, LEFT							
	9																
	10		10				1867452-7			TERMINAL							
	11																
	12	#	1	D			2797459-1			STATOR ASSY, MECHANICAL							
	13																
	14	#	AIR D				2797460-1 (APPROX 186 REQ)			LAMINATION, STATOR							
	15																
	16	#	68				2797461-1			BLOCK VANE							
	17	#	28				2797461-2			BLOCK VANE							
	18																
	19	#	B C				2797462-1			COIL ASSEMBLY							
	20																
	21	#	B C				2797463-1			BOBBIN							
	22		A/R				98412100000			WIRE, ELECTRICAL							
	23		MR				98412010000			WIRE, ELECTRICAL							
	B 24	#	2 B				2803990-1			INSULATOR							
	25		A/R				25 GAGE TYPE	PYRE-HML		WIRE, MAGNET							
	26																
	27																
	28	#	16 B				2797464-1			SPLINE							
	29																
	30	#	1 D				2797465-1			ROTOR							
	31																
	32	#	1 C				2797469-1			PLATE ASSEMBLY							
	33	#	1 F				2797473-1			PLATE MANIFOLD, LEFT							
	34	#	2 B				2797498-1			SPACER							
	35		2				92341060400			PIN, DOWEL							
	36																
	37	#	1 F				2797474-1			PLATE MANIFOLD RIGHT							
	38																
	39	#	1 F				2797471-1			PLATE, PNEUM TRANS, RIGHT							
	40	#	1 F				2797472-1			PLATE, PNEUM TRANS, LEFT							
	41																
	42																
	43																
	44																
	45																
	46																
	47	#	1 D				2797475-1			GASKET							
	48	#	1 D				2797475-2			GASKET							
	49																
	50																

THE BENDIX CORPORATION NAVIGATION & CONTROL GROUP TETERBORO, N. J. 07608				19315		LIST NUMBER PL 3854020-1												
REMARKS:				CODE IDENT SHEET 1 NUMBER 3		PREP: KENOBUE 1 MAY 78												
				CKD:														
IT. REV.	ITEM NO.	# NEW	REV	A	QTY REQ	SIZE	PART NO.	FIND NO.	VENDOR PART NO.	ASSEMBLY LEVEL						DESCRIPTION	REL NO.	
										1	2	3	4	5	6			
	1																	
	2	#	B	B			2797477-1											SHAFT ORBIT
	3	#	1	B			2797482-1											END SHAFT
	4																	
	5	#	1	D			2797478-1											GEAR RING
	6	#	1	C			2797479-1											GEAR FIXED SENSOR END
	7	#	1	C			2797480-1											GEAR FIXED OUTPUT END
	8	#	1	D			2797481-1											GEAR OUTPUT
	9																	
	10	#	2	B			2797482-1											SPACER THRUST BRG
	11	#	A/R	B			2797483-1											SHIM
	12	#	A/R	B			2797483-2											SHIM
	13	#	A/R	B			2797483-3											SHIM
	14																	
	15																	
	16	#	B	B			2797484-1											WAVE
	17																	
	18																	
	19	#	2	B			2797485-1											STOP
	20																	
	21	#	1	D			2797487-1											ARM, CEANR
	22																	
	23		2				IKO INTERNATIONAL	NTB-2542										BEARING NEEDLE THRUST
	24		2				TORRINGTON	WJ 404G16										BEARING FOLLER
	25		2				TORRINGTON	HJ 142216										BEARING ROLLER
	26																	
	27																	
	28		1				PICKERING	36510										SENSOR ANGULAR
	29																	
	30		16				MS1628-4025	TRUNC 5101-25										RING RETAINING
	31		2				RAMSEY (SPIROLOX)	UR-287-S										RING RETAINING
	32		1				MS9021-020											O RING
	33																	
	34		3	B			7116894-1											CLAMP COMPONENT
	35																	
	36		2				92341080500											DOWEL PIN
	37																	
	38							BENDIX										
	A39		1				MS27473RE(SR)16A99P	STOORE-16-99P(SR)										CONNECTOR
	40																	
	41		1	C			1591757-15											CLAMP CABLE
	42		1	A			1213459-2											WASHER, CABLE CLIP
	43																	
	44																	
	45																	
	46																	
	47																	
	48																	
	49																	
	50																	

BRUNING 26815

IT. REV.		ITEM NO.	#-NEW	REV	QTY REQ	SIZE	PART NO.	FIND NO.	VENDOR PART NO.	ASSEMBLY LEVEL						DESCRIPTION	REL NO.	
										1	2	3	4	5	6			
	1			2			NAS6204-24										BOLT, HEX HD	
	2			2			NAS6204-68										BOLT, HEX HD	
	3			1			NAS6204-23										BOLT, HEX HD	
	4			5			MS24674-3										SCREW, CAP, SOCK HD	
	5			5			MS24674-5										SCREW, CAP, SOCK HD	
	6																	
	7			1			MS24674-1										SCREW, CAP, SOCK HD	
	8			32			MS24674-11										SCREW, CAP, SOCK HD	
	9			1			92522020400										SCREW, CAP, SOCK HD	
	10																	
	11																	
	12			3			92552030400										SCREW, MACH, PAN HD	
	13																	
	14			3			92101030000										LOCKWASHER	
	15																	
	16			3			NAS1291CAM										NUT, SELF LOCKING, HEX	
	17																	
	18			A/R			MS20395-C32										LOCKWIRE	
	19																	
	20																	
	21																	
	22			A/R			98412100000										WIRE, ELECTRICAL	
	23																	
	24																	
	25																	
	26	#		1	F		2797500-1										SERVO VALVE ASSY.	
	27																(P.L. 2797500-1)	
	28																	
	29																	
	30			4			MS24673-5										SCREW, CAP, SOCK HD	
	31																	
	32			4			MS35338-138										LOCKWASHER	
	33																	
	34																	
	35																	
	36																	
	37																	
	38																	
	39						D 2797476										BLOCK DIAGRAM	
	40																	
	41																	
	42																	
	43																	
	44																	
	45																	
	46	#		A			2797496										PROCEDURE	
	47																	
	48	#		F			2797486										INSTALLATION DWG	
	49																	
	50																	

DRAWING 26615

THE BENDIX CORPORATION										LIST NUMBER						
NAVIGATION & CONTROL GROUP · TETERBORO, N. J. 07608										19315		PL 2797500-1				
REMARKS:										CODE IDENT		SHEET NUMBER 2				
										PREP: LEJ00UE		1-MAY 78				
										CKD:						
IT. REV.	ITEM NO.	#-NEW	REV	CTY REQ	SIZE	PART NO.	FIND NO.	VENDOR PART NO.	ASSEMBLY LEVEL						DESCRIPTION	REL NO.
									1	2	3	4	5	6		
	1	#	1	F		2797500-1									SERVO VALVE	
	2															
	3															
	4															
	5	#	1	C		2797489-1									VALVE MECH (MATCHED)	
	6															
	7															
	8	#	1	C		2797492-1									FLOW TRIM ASSY	
	9															
	10	#	1	F		2797491-1									BODY VALVE	
	11	#	1	D		2797492-1									SPool	
	12	#	1	B		2797493-1									ROD, GUIDE	
	13															
	14					MS16628-40LS									RING RETAINING	
	15					MS16624-40LS									RING, RETAINING	
	16															
	17															
	18	#	1	C		2797494-1									CAP END	
	19	#	1	C		2797495-1									CAP, END	
	20															
	21		2			THOMSON	#	XA-4812-SS							BALL BUSHING	
	22															
	23		2			MS16629-4050									RING RETAINING	
	24		2			MS16625-4050									RING RETAINING	
	25															
	26		2			MS9021-30									O" RING	
	27															
	28	#	1	B		2797466-1									CAP	
	29															
	30	#	1	B		2797467-1									BRACKET	
	31															
	32	#	1	B		2797468-1									ROD OPERATING	
	33															
	34	#	1	D		2797469-1									BRACKET, MOUNTING	
	35	#	1	C		2797470-1									COVER	
	36															
	37	#	1	B		2797497-1		SERVOTRONICS #21-4 (MODIFIED)							TORQUE MOTOR	
	38															
	39					MS16628-40LS									RING RETAINING	
	40		2			MS16624-40LS									RING, RETAINING	
	41															
	42		1			SCHAEVITZ	#	O25MHR							TRANSDUCER	
	43															
	44															
	45															
	46															
	47															
	48															
	49															
	50															

IT. REV.		ITEM NO.	#-NEW	REV	A	CTY REQ	SIZE	PART NO.	FIND NO.	VENDOR PART NO.	ASSEMBLY LEVEL						DESCRIPTION	REL NO.	
												1	2	3	4	5	6		
	1			3				MS24673-1			SCREW, CAP, SOCK HD								
	2			6				MS24673-2			SCREW, CAP, SOCK HD								
	3			10				MS24677-1			SCREW, CAP, SOCK HD								
	4			2				MS24677-3			SCREW, CAP, SOCK HD								
	5																		
	6																		
	7																		
	8			2				MS51960-65			SCREW, HIGH, FLAT CSUNK								
	9																		
	10																		
	11			1				MS51021-15			SCREW, SET, CUP POINT								
	12																		
	13																		
	14			3				AN960-C10L			WASHER, FLAT								
	15																		
	16																		
	17																		
	18			A/R				MS20995-C32			LOCKWIRE								
	19																		
	20																		
	21																		
	22																		
	A 23			1				MS27473RE(SR)12A98P		BENDIX JTO6RE-1298P(SR)	CONNECTOR, ELECT.								
	24																		
	25																		
	26																		
	27																		
	28																		
	29																		
	30																		
	31																		
	32																		
	33																		
	34																		
	35																		
	36																		
	37																		
	38																		
	39																		
	40																		
	41																		
	42																		
	43																		
	44																		
	45																		
	46																		
	47																		
	48																		
	49																		
	50																		

REPORT NADC 82047 60

DISTRIBUTION LIST

AIRTASK 62241N-F41400

	<u>NO. OF COPIES</u>
NAVAIRSYSCOM (AIR 950 D) Washington, DC 20361	5
2 for Retention	
2 for AIR 340 D	
1 for AIR 53014C2	
NAVAIRDEVGEN (60134) Warminster, PA 18974	41
3 for 813	
1 for 30	
1 for 60	
1 for 60C	
1 for 601	
1 for 6012	
1 for 6013	
32 for 60134	
AFFDL Wright Patterson AFB, Ohio 45433	2
Defence Technical Information Center Cameron Station, Alexandria, VA 22314	12
Rockwell International NAAD Columbus, Ohio 43216	5
Bendix Corporation	<u>10</u>
TOTAL	75

DATE
ILME